NASA CONTRACTOR REPORT

NASA CR-88

NASA CR-88

HYPERSONIC MAGNETOHYDRODYNAMICS WITH OR WITHOUT A BLUNT BODY

by R. H. Levy, P. J. Gierasch and D. B. Henderson

Prepared under Contract No. NASw-748 *by*
AVCO CORPORATION
Everett, Mass.
for

NATIONAL AERONAUTICS AND SPACE ADMINISTRATION • WASHINGTON, D. C. • JULY 1964

HYPERSONIC MAGNETOHYDRODYNAMICS WITH OR WITHOUT A BLUNT BODY

By R. H. Levy, P. J. Gierasch and D. B. Henderson

Prepared under Contract No. NASw-748 by
AVCO CORPORATION
Everett, Mass.

for

NATIONAL AERONAUTICS AND SPACE ADMINISTRATION

For sale by the Office of Technical Services, Department of Commerce,
Washington, D.C. 20230 -- Price $2.00

TABLE OF CONTENTS

ABSTRACT

25968

We consider the hypersonic flow of a cold gas past a two-dimensional or axially symmetric body containing a two or three-dimensional magnetic dipole with its axis oriented parallel to the flow. The magnetic moment of the dipole and the size of the body are of arbitrary proportions. A uniform scalar conductivity is turned on by the shock, and the magnetic Reynolds number is low. For low values of the interaction parameter the flow is quasi-aerodynamic. Certain discrepancies existing in the literature on the flow in this regime are reconciled. At high values of the interaction parameter the nature of the flow is quite different. In this regime it consists of a thin deceleration layer (somewhat akin to the aerodynamic shock layer) and an extensive region of low Mach number flow (called the slow flow region) which separates the deceleration layer from the body. The gas in the slow flow region escapes outward at sonic velocity along the field lines. In some circumstances the entire flow field can be supported by the magnet, i. e., without the hot gas touching the body. Assuming a large compression ratio across the shock a relatively simple analysis can be performed. Calculations covering various representative cases are exhibited; the validity and significance of these calculations are discussed.

author

NOMENCLATURE

$x, y, r, \theta, R, \phi, n, s, \tilde{r}, \tilde{n}, \xi$	various coordinates
u, v	velocity components
p	pressure
ρ	density
B	magnetic field
B_r, B_θ, B_s, B_n	various magnetic field components
j	current density
σ	conductivity
ψ	stream function
S	interaction parameter
ϵ	limiting shock compression ratio
$r_c, r_s, r_b, \Delta, \delta, a$	various distances
κ	curvature
k	reference pressure gradient
η	magnetic field line parameter
I, M, P	integral quantities
t	dummy variable
Q_0, Q_1, α	auxiliary quantities
G, g, h, f_1, f_2	auxiliary functions
F	hypergeometric function
subscripts	
0	reference quantity
∞	free stream value
M	matching
L	deceleration layer

I. INTRODUCTION

The interaction between a hypersonic flow and a fixed magnetic field is of interest in a number of connections. While such an interaction can take place in a variety of physical conditions, we shall, in this paper, consider only the case in which the magnetic Reynolds number is negligibly low. It is most appropriate (for the applications we have in mind) to consider the smallness of the magnetic Reynolds number as due to a low value of the conductivity of the working gas. One great simplification which results from considering the magnetic Reynolds number to be low is that the complicated wave propagation effects characteristic of magnetohydrodynamics at high magnetic Reynolds number disappear in our limit. In fact we can regard our flows as entirely aerodynamic in structure, although differing from traditional types of aerodynamic flows in that the applied forces act through a volume rather than at surfaces. In addition to assuming the magnetic Reynolds number small, we shall suppose that the conductivity of our gas will be "turned on" by a strong bow shock wave. This assumption corresponds to the conditions encountered in hypersonic flight in planetary atmospheres. We shall see later on that it will be legitimate to consider this conductivity as a constant over an interesting part of the flow field.

Now, the general conditions described above have formed the basis of quite a few studies. For our purposes we can distinguish two groups of such studies, namely, those in which the flow is considered to be primarily aerodynamic and is modified by the magnetic field, and those in which the flow is dominated by the magnetic interaction and the presence of a body is of secondary importance. We shall be concerned in this paper with the latter category, and will emphasize in particular those flows in which forces exerted at solid surfaces play a negligible role. However, it will be useful briefly to review both categories of studies in order to establish a perspective.

A group of papers by Kemp,[1] Bush[2] and Lykoudis[3] deals with the hypersonic flow of gas over a body and the modification of this flow by a magnetic field. The points of difference between these papers are largely in the choice of method, the actual problem being in all cases just about the same. While not explicitly stated in all the papers, the general idea is that the magnetic forces are less than those exerted at the surface of the body. Bush, however, does suggest the possibility of the opposite extreme. The results of all these papers are given in terms of calculated modifications of the aerodynamic flow. Thus the effect of the magnetic field is to reduce the stagnation point velocity gradient, to increase the shock stand-off distance, and therefore to reduce the convective stagnation point heat transfer. The drag is largely unaffected.

A different approach is given in a paper of Levy and Petschek.[4] Here a rather special two-dimensional problem is studied with a view to describing a flow in which the body is entirely absent. The nature and existence of such flows was demonstrated. The results of such a study clearly cannot be stated with reference to any standard aerodynamic flow. Rather, such parameters as the location of the shock are given in terms, for instance, of the current flowing in the magnet. An important feature of this type of flow is the existence of an inner boundary to the flow behind which the gas density is very low. If the body which houses the magnet is inside this inner zone, it is essentially not in contact with the flow at all, and the convective heat transfer to it should be very small.

In the present paper we attempt to combine features of both the above problems. The geometry we study is the physically realistic geometry of the first group of papers, but we use the methods of Levy and Petschek and concentrate strongly on the case in which the body plays a negligible role in the flow. In the course of the work certain discrepancies existing in the first group of papers are resolved, and the flow corresponding to the limit discussed by Bush is extensively described. More particularly, in the next section we specialize the configuration to be studied and describe the main outlines of our analysis. In subsequent sections we will analyze the flow in greater detail, and discuss particularly the limiting cases in

which the flow is principally supported by either the magnetic field or the body. In the last section we will draw some general conclusions from our study, and also describe some of the physical limitations on the validity of our analysis.

II. GENERAL DESCRIPTION OF THE FLOW

We consider the hypersonic flow of a cold gas past a two-dimensional or axially symmetric body containing a two or three-dimensional magnetic dipole with its axis oriented parallel to the flow. The general features of this flow are illustrated in Fig. 1. A strong shock will be formed in the gas ahead of the object; behind this shock the gas is weakly conducting. In the axially symmetric case the current flow (in the absence of Hall effect) is in the azimuthal direction and it follows that $\underset{\sim}{j} \cdot \underset{\sim}{E} = 0$. In the two dimensional case this condition can also be achieved if we suppose the body to form a ring whose major radius is much greater than any dimension of its cross section. The importance of this condition is due to the fact that where it is not satisfied, energy can be transferred from one streamline to another (one acting as a "generator," the other as a "motor"). Such transfers of energy cannot take place in the absence of induced or applied electric fields; thus, in our case, each streamline is isolated energetically and, therefore, has a constant total enthalpy. We neglect heat conduction and viscosity since the viscous Reynolds number is high; when there is no body in the flow there will not even be a thin viscous boundary layer. Since the total enthalpy is constant along each streamline, it is constant throughout the flow. In the region where the Mach number is low (behind the normal part of the shock, for example) the static enthalpy will be approximately constant. We shall assume that the properties of the gas are such that the electrical conductivity may be treated as constant when the enthalpy is constant, even though the gas may undergo a considerable expansion. This assumption will allow us to take the conductivity as constant through a large part of the flow. We also assume that the gas conditions are such that the Hall effect may be neglected; in the last section we shall estimate limits to the validity of this assumption.

The statement that the gas is weakly conducting behind the shock is to be taken to mean that the magnetic Reynolds number is low. The general

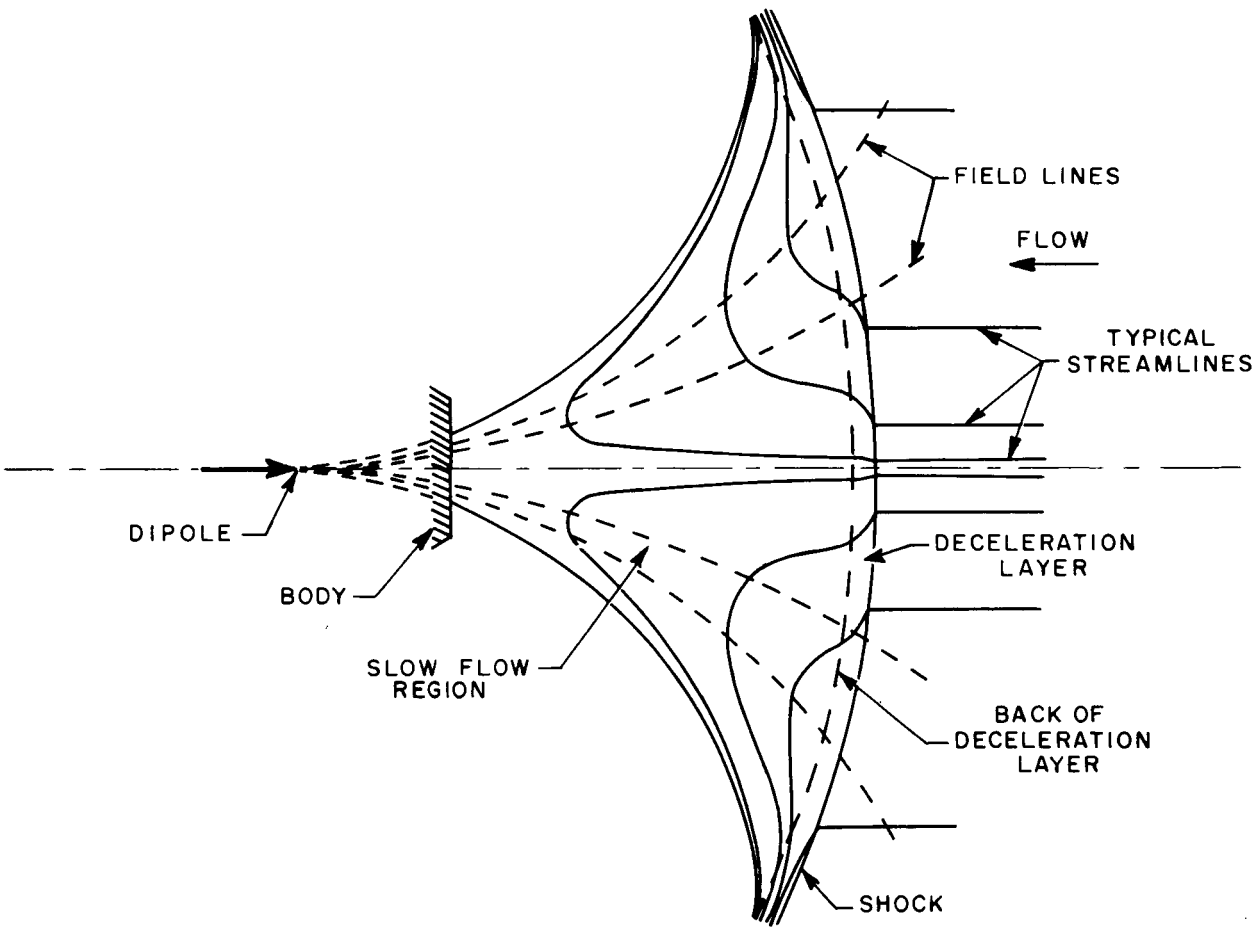

Fig. 1 Illustrates the principal features of the flow to be expected when $S \approx 1$. The conductivity is zero ahead of the shock.

features of flows at low magnetic Reynolds numbers have been outlined elsewhere, but for the sake of completeness we include a brief description here. When the magnetic Reynolds number is low, the currents induced in the gas give rise to magnetic fields which are negligible in comparison to those due to the primary field coils. Thus, the magnetic field at any point in the flow can be calculated as though it were due only to the field coils. At the same time, in order to have a substantial exchange of momentum between the field and the flow the magnetic pressure must be much greater than the dynamic pressure of the flow. More detailed analysis shows that, when a substantial interaction is present (which is certainly the case when there is a strong shock), the product of the magnetic Reynolds number and the ratio of the magnetic to dynamic pressures must be of order unity. We call this product the interaction parameter, and denote it by S. Of course, careful attention must be paid to the designation of the characteristic quantities that go into it.

The geometrical configuration shown in Fig. 1 is generically the same as that treated by Bush et al. The magnetic field will be that due to a two-dimensional or axially symmetric dipole whose axis is in the flow direction. The body will generally be blunt. In two dimensions we consider cylinders of arbitrary cross section, but having a plane of symmetry in which the dipole is located. In three dimensions we consider arbitrary axially symmetric shapes. In general we do not assume that we have circular cylinders or spheres, although we could treat these shapes as special cases. The location of the dipole is, within the limitations of symmetry, arbitrary, except that it is supposed not to be right at the stagnation point of the body. Also, we do not make any a priori assumption about the shape or the location of the shock.

We define ϵ to be the reciprocal of the limiting compression ratio across strong shocks for the gas and conditions under study. It is frequently a small number in practice, and we shall assume throughout the analysis that $\epsilon \ll 1$. Now, in aerodynamics, this assumption leads directly to the flow picture generally (if somewhat roughly) described as Newtonian. In

the analysis of Newtonian flows, the shock layer (the thin region between the shock and the body) is generally not resolved in detail. The gross mass and momentum fluxes are balanced, however, in various different ways.[5] Now for magnetohydrodynamics, this description is not adequate since the detailed velocity of the gas across the field lines must be known in order to find the resultant magnetohydrodynamic body force. We must therefore use a Newtonian description of the flow which nevertheless provides a consistent representation of the flow velocity, and especially the component of the flow velocity normal to the magnetic field.

We define the deceleration layer (see Fig. 1) as the region just behind the shock for which the velocity component parallel to the shock is larger than the component normal to the shock. (The deceleration layer reduces, when there is no magnetic interaction, to the aerodynamic shock layer. The reason for this choice of terminology will become apparent later on.) Although this definition breaks down near the place where the shock is normal, it can be extended in a consistent manner to the stagnation streamline by using the gradient of the velocity component parallel to the shock, multiplied by the radius of curvature of the shock. The important thing to conclude from this definition is that, due to the requirement of continuity, the deceleration layer as defined is thin. In fact, since the ratio of the velocity components perpendicular and parallel to the shock is on the order of ϵ, the continuity equation tells us that the thickness of the layer is approximately ϵr_c, where r_c is the radius of curvature of the shock. Note that the demonstration that the deceleration layer is thin depends only on the properties of shocks and the conservation of mass.

Now toward the front of the deceleration layer, near the shock, the pressure gradient along the layer exerts a negligible effect on the flow. In the aerodynamic case, this means that the tangential component of velocity of each fluid particle is conserved as it follows a streamline. This in turn means that as we traverse the layer from front to back, we encounter particles carrying less and less tangential velocity. In the limit, on this theory, the dividing (stagnation) streamline would have no tangential velocity. This conclusion is incorrect and, in fact, we have to take account of

the pressure gradient along the layer for those particles which crossed the shock at an angle less than about $\epsilon^{1/2}$ from the normal and which subsequently form the back of the layer. Knowing that we have to take the transverse pressure gradient into account in this region, we consider how to calculate it. Now the transverse pressure gradient is clearly known at the shock. For the aerodynamic case, the only effect capable of changing this pressure gradient across the layer is the centrifugal force which acts outward, and hence reduces the pressure at the back of the layer; this reduction in pressure away from the stagnation point has the effect of increasing the magnitude of the stagnation point pressure gradient. But the only important contributor to the centrifugal effect is the high velocity gas at the front of the layer and it is precisely this gas which is unaffected by the transverse pressure gradient. Therefore, we can calculate the centrifugal effect neglecting the effect of the pressure gradient and then find the change in the pressure gradient due to the centrifugal effect. Put another way, we first calculate the flow in the layer neglecting the effect of the tangential pressure gradient. The resulting velocities are incorrect only where they are low, so that the centrifugal effect can be deduced from them without substantial error. We then calculate the pressure gradient throughout the layer as modified by the centrifugal effect. The final step is to evaluate the pressure gradient calculated in this way at the back of the layer and treat this value as though it were correct throughout the layer. This step is incorrect near the shock, where it has no effect, but is correct at the back, where it is important. We shall see later on how this procedure, generalized to the magnetohydrodynamic case, covers correctly the aerodynamic limit.

The extension of this scheme to the magnetohydrodynamic case proceeds as follows: We commence, as before, by neglecting the pressure gradient in the transverse momentum equation. The tangential velocity of each particle is now, however, not constant along a streamline, but is reduced by the interaction with the magnetic field. (See Fig. 1). This leads to an interesting situation; apart from extremely small values of the interaction parameter (just how small will be discussed in due course) the transverse component of the velocity at some distance back from shock may fall to low values before we reach the body (the body is where the radial velocity

vanishes). By our definition, the place where the two components are comparable in magnitude is the back of the deceleration layer. Thus, in the magnetohydrodynamic case, there may be an outflow from the back of the deceleration layer. There is, therefore, an additional flow region behind the deceleration layer which will have to be studied in order to complete the solution to the whole flow problem. In view of the fact that in this region both velocity components are of order ϵu_∞, we shall refer to it as the "slow flow region." Since the Mach number is very low, the convection of momentum in it will be negligible compared to the pressure gradients and the magnetohydrodynamic forces. The balance of these last two therefore determines the nature of the flow. Two additional remarks concerning the slow flow region are important. First, since the velocity components in both directions are comparable, the equation of continuity shows that the dimensions of the slow flow region are roughly comparable in all directions. Secondly, since there is no magnetohydrodynamic force along the field lines the pressure is a given constant for each field line.

Now, in order to solve the flow in the slow flow region, we must know, from study of the deceleration layer, the pressure on each field line, and the flow velocity across the boundary between the regions. We have shown how to calculate the latter and it remains to determine the pressure at the back of the layer. To accomplish this we proceed in a manner entirely analogous to the method used in the aerodynamic case. We note that the forces normal to the deceleration layer capable of changing the pressure between the front and the back are the centrifugal force (as before) and, in addition, the normal component of the magnetohydrodynamic force. Once again, both of these are significant only where the tangential velocity is high, and we can therefore use the tangential velocity profile calculated neglecting the pressure gradient to find the net loss of pressure through the layer. This procedure is quite straightforward, but can give rise to effects of different signs. In the first place the tangential velocity is always reduced below its aerodynamic value by the magnetic field. Thus, the centrifugal effect is always less than in the aerodynamic case. On the other hand, the normal component of the magnetohydrodynamic force can have either

sign. Since it is always normal to the field lines, the force acts outward (in concert with the centrifugal force) or inward (against the centrifugal force) according as the field lines appear locally to diverge from a point ahead of or behind the center of curvature of the deceleration layer. These remarks explain the difference in the sign of the change in the body pressure gradient in the work of Kemp and Bush. Kemp has a pole at the center of curvature of the deceleration layer. There is thus no component of the magnetic force normal to the deceleration layer. The only effect on the pressure is, then, that the centrifugal effect is reduced. As a result, the pressure at the body is higher than in the aerodynamic case, and the stagnation point pressure gradient is reduced. Bush, on the other hand, has a dipole at the center of curvature of the shock layer. Thus, the magnetic force is outward, the pressure on the body is reduced, and the stagnation point pressure gradient is increased.

While Kemp, Bush and Lykoudis refer exclusively to the pressure gradient on the body, our results refer quite generally to the back of the deceleration layer, that is, whether or not it is separated from the body by a slow flow region. We now estimate the value of the interaction parameter above which a slow flow region intervenes between the deceleration layer and the body. Before doing this, however, it is convenient to define more precisely the interaction parameter to be used throughout the paper. We let

$$S = \epsilon \sigma B_o^2 r_c / \rho_\infty u_\infty \tag{2.1}$$

where B_o is the field strength at the normal point of the shock. Now it is clear that as long as the magnetohydrodynamic force has an effect on the transverse (or tangential) momentum equation comparable to that of the tangential pressure gradient, the deceleration layer will be only slightly changed from the aerodynamic case. This is because, as we have seen, the tangential pressure gradient does not affect the aerodynamic shock layer very much anyway. This condition gives us:

$$\sigma u_\infty B_o^2 \approx \rho_\infty u_\infty^2 / r_c \tag{2.2}$$

where the left hand side is the characteristic magnetohydrodynamic body force in the transverse direction and the right hand side is a pressure gradient made up from a change in pressure comparable to free stream dynamic distributed over a distance like the radius of curvature of the deceleration layer. Using the definition (2.1), (2.2) becomes

$$S \approx \epsilon \tag{2.3}$$

On the other hand, when the magnetic force is capable of stopping the transverse flow in the deceleration layer, we can expect that the normal velocity will not reach zero in the layer, and that a slow flow region will be necessary. This condition occurs when

$$\sigma u_\infty B_o^2 \approx \frac{\rho_\infty}{\epsilon} \frac{u_\infty^2}{r_c} \tag{2.4}$$

The right hand side here is the volume force necessary to stop gas having density ρ_∞/ϵ and velocity u_∞ during the time it is in the deceleration layer, namely r_c/u_∞. Using (2.1), (2.4) becomes

$$S \approx 1 \tag{2.5}$$

Between these limits, then, the slow flow region makes its appearance. We shall see later, on the basis of more detailed considerations, that the critical value of S is given by

$$S \approx \epsilon^{1/2} \tag{2.6}$$

When $S\epsilon^{-1/2} \ll 1$ the magnetic field has less effect on the flow than the pressure gradient. We can, therefore, make the following statements about the flow in this regime: The flow takes place entirely within a deceleration layer whose thickness will be slightly greater than, but of the same general order of magnitude as the aerodynamic shock layer on the same body, i.e. ϵr_c. Likewise, the stagnation point velocity gradient continues to be on the order of $\epsilon^{1/2} u_\infty r_c^{-1}$, but is slightly reduced by the magnetic interaction. In general it will always be reasonable to compare the features of the flow in this regime with the corresponding features of the pure aerodynamic flow around the same body.

The situation pertaining when $S \gg \epsilon^{1/2}$ is entirely different. The deceleration layer is now no longer in contact with the body, but is separated from it by the slow flow region. There is no longer any justification for assuming that the layer is concentric with the body, or, for that matter, with the dipole. Whatever the geometry, the type of flow we expect is illustrated schematically in Fig. 1. The pressure at the back of the deceleration layer is reduced by the combined action of the centrifugal and magnetic forces. At the same time the component of velocity parallel to the deceleration layer at the back of the layer rises as we proceed away from the stagnation streamline; the gradient of this velocity component where the deceleration layer is normal is $\epsilon u_\infty r_c^{-1}$, but it will subsequently grow more rapidly when the angle between the field and the deceleration layer becomes small. At some point it will reach sonic velocity $\epsilon^{1/2} u_\infty$. At this point the flow in the "slow flow region" can no longer be slow. On the other hand, flow that entered the slow flow region near the axis can be expected to escape at higher speed in the general direction of the magnetic field. The analysis of this flow is beset with a number of difficulties. Thus, as the velocity rises, the temperature and hence the conductivity will fall; furthermore, the density will also be lower away from the stagnation streamline; at some point nonequilibrium, Hall, and ion-slip effects must all become important. Two methods are available at this stage. The first, used by Bush (and others) is to introduce the ad hoc assumption that the dipole is at the center of curvature of the shock wave. No justification of this assumption seems possible, but it does lead to a definite problem which can be solved without discussing the tricky matter of the nature of the flow near the sonic points. The second alternative is to construct a satisfactory model of the flow out to the sonic point. In this paper we adopt the second alternative; we shall see, however, that in order to construct this flow we are obliged to make assumptions about gas properties that are not too well justified in practice. An important result of our analysis will be a reasonable degree of agreement between our results and those of Bush. Since the results are obtained by different methods, it is felt that each lends support to the other.

The model of the flow away from the stagnation streamline is then as follows: Gas that enters the slow flow region near the axis has a characteristic velocity ϵu_∞. It is accelerated outward along the field to sonic velocity $\epsilon^{1/2} u_\infty$. Assuming the motion to be isothermal, the density will decrease only to about $e^{-1/2}$ of its stagnation value, so that the area required to pass the sonic flow out at sonic velocity is only about $\epsilon^{1/2}$ of the area over which it entered. This area on our assumption is very small. At the same time, the velocity at the back of the deceleration layer can be sonic when the j x B force is reduced to something comparable to the pressure gradient. When this happens, it can be shown that the component of the magnetic field normal to the layer must be reduced to a fraction $\epsilon^{1/4}$ of its value at the stagnation point. Thus, the deceleration layer is essentially parallel to the magnetic field. Finally, the pressure at the back of the layer is much reduced by the centrifugal effect. We suppose that, at a certain point along the layer 1) the layer becomes parallel to the magnetic field; 2) the pressure at the back of the layer is reduced to nothing by the centrifugal effect, and 3) the slow flow gas, having been accelerated to sonic velocity along the field, constitutes a thin back edge at the back of the deceleration layer. These features are shown schematically in Fig. 1. A particularly important feature of Fig. 1 is the existence of a limiting field line which is also a streamline, beyond which the flow does not penetrate. As can be seen, this implies that only a definite area near the stagnation point of the body is in contact with the flow, and that away from this point the pressure and density, and hence the momentum and heat transferred to the body, rapidly decline, reaching zero where the body intersects the limiting field line.

It can be seen that the model of the flow just described depends for its validity on the assumption $\epsilon^{1/4} \ll 1$. This assumption is far stronger than the simple $\epsilon \ll 1$ and is, in fact, not very well satisfied in practice. This remark clearly limits the validity of our model.

All of the above remarks apply to the case $S\epsilon^{-1/2} \gg 1$. Throughout most of this range, a body is present, as shown in Fig. 1. However, for sufficiently large S, of order unity, we reach a very interesting situation

in which the body vanishes altogether (except for the stagnation point!) and the whole drag of the flow field is felt by the magnetic field coil. Beyond this point, as observed by Bush, no further increase in S is possible. An increase of the magnet strength, for instance, results only in the shock moving further away from the magnet. Obviously, this situation, if it can be realized, offers prospects of heat transfer reduction greatly in excess of those demonstrable in the range $S\epsilon^{-1/2} \ll 1$. The situation does, however, depend to some extent on the validity of our model. While this important result may be considered to be implicit in the work of Bush, it was not pointed out there; clearly, in order to understand it, some treatment of the flow away from the stagnation streamline is necessary. This point will be dealt with following a more detailed analysis of the flow model.

For the case in which $S\epsilon^{-1/2} \gg 1$ we lack simple solutions for the flow in the deceleration layer away from the stagnation streamline. We, therefore, use an integral method with assumed profiles, and we can in principle, proceed in two ways. For various shapes of the layer and locations of the dipole we can find the body, and for various bodies we can find the layer. Because of its greater difficulty we use the latter method only to find the shock corresponding to no body.

The organization of our analysis is as follows: In Section III we study the flow in the deceleration layer near the stagnation streamline. In Section IV we study the flow in the entire slow flow region. In Section V we match these two solutions at the back of the deceleration layer on the stagnation streamline, and reach certain conclusions about the relation between S, r_c and the locations of the body and the dipole. At this stage it will be clear how the ad hoc geometrical assumption of Bush makes the problem soluble, and what its implications are. In Section VI we study the deceleration layer away from the stagnation streamline by the momentum integral method. In Section VII we discuss the results of numerical calculations in which the slow flow is matched to the deceleration layer along its entire length for various representative cases. The last section, Section VIII, contains conclusions relevant to the analysis as a whole, and a general discussion of its validity and implications.

III. DECELERATION LAYER ANALYSIS IN THE STAGNATION REGION

We commence our detailed analysis of the flow problem in that part of the deceleration layer which is close to the place where the shock is normal. We fix coordinate systems as shown in Fig. 2. Taking as origin the center of curvature of the shock at the point where it is normal, we define Cartesian coordinates (x, y) such that the undisturbed flow is in the negative x-direction, and polar coordinates (r,θ).* The radius of curvature itself is r_c. The velocity components (u, v) are defined to be in the direction of increasing (r, θ), that is, they are based on the polar coordinates measured from the center of curvature of the shock. The dipole is located inside some cylindrical body; the distance from the dipole to the front of the body is r_b. We define a second system of polar coordinates (R,ϕ) based on the dipole as origin. Other dimensions are shown in Fig. 2.

We non-dimensionalize all the flow quantities in accordance with the general picture of the flow in the deceleration layer developed in the preceding section. Thus, the pressure is non-dimensionalized with the free

---

* In this section, and in what follows, we shall describe in the text the cylindrical problem only. The axially symmetric problem is identical in logical derivation, but differs in algebraic detail. Therefore, we have relegated to Appendix A all discussion of this case, and all equations relevant to it that differ from those of the cylindrical (two-dimensional) case. The notations are as nearly identical as possible, but some symbols will have slightly different meanings for the two cases. Thus (r, θ) will be used for both the spherical and the cylindrical polar coordinate systems referred to the center of curvature of the normal part of the shock. Also, we have numbered the equations in Appendix A not consecutively, but to correspond to the same equation written for the two-dimensional case, as these will be numbered in this and subsequent sections. Finally, where the Figures differ for the two cases, we exhibit both reserving "a" for the cylindrical case and "b" for the axially symmetric case.

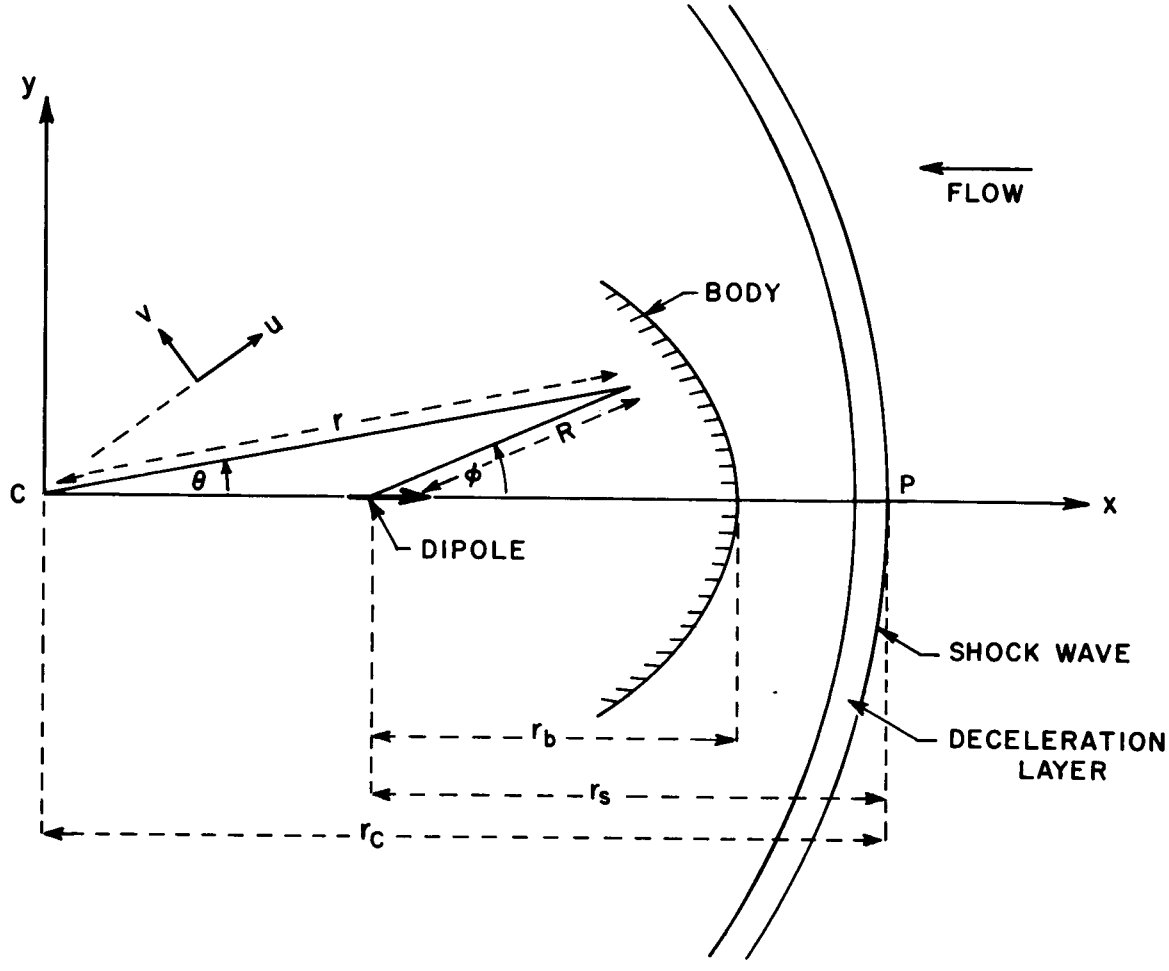

Fig. 2 Illustrates the coordinate systems used in the text. C is the center of curvature of the deceleration layer at the point P. The components (u, v) of the velocity are polar, and are referred to the coordinate system (r,θ) with origin at C.

stream dynamic pressure, $\rho_\infty u_\infty^2$, the density with the density behind a strong shock, ρ_∞/ϵ, all distances with the radius of curvature of the shock, r_c, the velocity components in the radial and tangential directions with ϵu_∞ and u_∞, and the magnetic field with the field at the point where the shock is normal B_o. In addition, since the deceleration layer is of thickness ϵr_c, we introduce the expanded coordinate $\tilde{r}$, defined by

$$\tilde{r} = \frac{1}{\epsilon}\left(1 - \frac{r}{r_c}\right) \tag{3.1}$$

so that $\tilde{r} = 0$ at the shock and is of order unity at the back of the layer. In the deceleration layer we shall neglect $1/r$ compared with $\partial/\partial r = (-1/\epsilon r_c)(\partial/\partial\tilde{r})$. We also neglect the change in the field components across the layer.

The energy equation, as has already been explained, has for an integral the condition of constant total enthalpy throughout the flow. We shall suppose the gas to be so close to perfect that the enthalpy may be taken to be proportional to p/ρ. Then, with the non-dimensionalization described above, the energy equation reduces to

$$p = \rho(1 - v^2) \tag{3.2}$$

v, B_θ and j are odd functions of θ, and all other quantities are even functions of θ. Hence, on the stagnation streamline $\theta = 0$,

$$p = \rho \tag{3.3}$$

The equation of continuity is:

$$\frac{\partial(\rho u)}{\partial\tilde{r}} = \frac{\partial(\rho v)}{\partial\theta} \tag{3.4}$$

On the stagnation streamline this reduces to

$$\frac{d(\rho u)}{d\tilde{r}} = \rho\frac{\partial v}{\partial\theta} \tag{3.5}$$

The quantities appearing in (3.3) and (3.5) are regarded as functions of $\tilde{r}$ only. This method gives the appearance of treating the stagnation

streamline by itself, but it is in fact no different in principle from the methods common in aerodynamics[6] involving expansions in powers of θ. Its advantage lies in a clearer identification of the necessary assumptions.

The current (non-dimensionalized with $\sigma u_\infty B_o$) is given by:

$$j = \epsilon u B_\theta - v B_r \tag{3.6}$$

This is the appropriate form of Ohm's law.

On the stagnation streamline we have

$$\frac{\partial j}{\partial \theta} = \epsilon u \frac{\partial B_\theta}{\partial \theta} - \frac{\partial v}{\partial \theta} B_r \tag{3.7}$$

We shall assume that $\partial B_\theta / \partial \theta$ is much less than $\epsilon^{-1} B_r$. This condition implies only that the dipole is not located right at the back of the deceleration layer. It is the restriction on the position of the dipole mentioned in the last section. A result of this assumption is that we may take the current in the deceleration layer to be given on the stagnation streamline by:

$$\frac{\partial j}{\partial \theta} = - \frac{\partial v}{\partial \theta} \tag{3.8}$$

The radial momentum equation reduces in the deceleration layer to:

$$\rho v^2 + \frac{\partial p}{\partial \tilde{r}} + S B_\theta v = 0 \tag{3.9}$$

Note that the only term proportional to the inertia of the gas to be retained in (3.9) is the centrifugal one. The remaining terms are all negligible since in the region under consideration the Mach number is very low.

Since we may assume $B_r = 1$ in this region, on the stagnation streamline this gives

$$\frac{dp}{d\tilde{r}} = 0 \tag{3.10}$$

for which the appropriate integral is

$$p = 1 \tag{3.11}$$

Thus, to this approximation, the pressure on the stagnation streamline is constant. From (3.3) we immediately deduce, also for the stagnation streamline.

$$\rho = 1 \tag{3.12}$$

Applying this to the continuity equation as written for the stagnation streamline, (3.5) gives

$$\frac{du}{d\tilde{r}} = \frac{\partial v}{\partial \theta} \tag{3.13}$$

As indicated before, we shall also use (3.9) to deduce the pressure gradient at the back of the shock layer, when we have found a suitable profile for v. We therefore differentiate it twice with respect to θ, and set $\theta = 0$ to find: (since $\rho = 1$)

$$\frac{d}{d\tilde{r}} \left(\frac{\partial^2 p}{\partial \theta^2}\right) = -2 \left(\frac{\partial v}{\partial \theta}\right)^2 - 2S \frac{\partial B_\theta}{\partial \theta} \frac{\partial v}{\partial \theta} \tag{3.14}$$

We shall return to this equation in due course. The tangential momentum equation in the deceleration layer is:

$$\rho \left[-u \frac{\partial v}{\partial \tilde{r}} + v \frac{\partial v}{\partial \theta}\right] + \epsilon \frac{\partial p}{\partial \theta} + Sv = 0 \tag{3.15}$$

On the stagnation streamline this reduces (after differentiation with respect to θ) to:

$$-u \frac{d}{d\tilde{r}} \left(\frac{\partial v}{\partial \theta}\right) + \left(\frac{\partial v}{\partial \theta}\right)^2 + \epsilon \frac{\partial^2 p}{\partial \theta^2} + S \frac{\partial v}{\partial \theta} = 0 \tag{3.16}$$

As explained before, we can neglect the pressure gradient in this equation as long as we do not integrate beyond the point where the other terms become comparable to the pressure gradient. Thus:

$$-u \frac{d}{d\tilde{r}} \left(\frac{\partial v}{\partial \theta}\right) + \left(\frac{\partial v}{\partial \theta}\right)^2 + S \frac{\partial v}{\partial \theta} = 0 \tag{3.17}$$

This must be solved, together with (3.13). The boundary conditions at the shock are:

$$u = -1, \quad \frac{\partial v}{\partial \theta} = 1 \quad \text{when } \tilde{r} = 0 \tag{3.18}$$

We write the equations in the form:

$$\frac{\partial v}{\partial \theta}\,\frac{d\tilde{r}}{u} = \frac{du}{u} = \frac{d\left(\frac{\partial v}{\partial \theta}\right)}{\frac{\partial v}{\partial \theta} + S} \tag{3.19}$$

Hence:

$$-u = \frac{\frac{\partial v}{\partial \theta} + S}{1 + S} \tag{3.20}$$

and

$$\left.\begin{aligned} -u &= \left[e^{-(1+S)\tilde{r}} + S\right]/(1+S) \\ \frac{\partial v}{\partial \theta} &= e^{-(1+S)\tilde{r}} \end{aligned}\right\} \tag{3.21}$$

These equations show the principal features of the behavior of the flow in the deceleration layer as outlined in the previous section. The inward radial velocity tends to the limit $S/(1+S)$ while the tangential velocity decreases without limit as we approach the back of the layer. In order to find the back of the deceleration layer, we use the profile of (3.21) in (3.16) and see at what point the equation is no longer the balance between two terms both larger than the pressure gradient term. Substitution shows that we must distinguish two cases:

a) If S is small, (3.16) can be considered as a balance between the two convective terms. This is the aerodynamic limit. At a distance $\tilde{r} \approx -\frac{1}{2}\ln\epsilon$, $\partial v/\partial\theta \approx \epsilon^{1/2}$ and the pressure gradient becomes important. At this point $-u \approx \epsilon^{1/2} + S$.

b) If S is large (3.16) can be considered as a balance between the first of the two convective terms and the magnetic term. This is the magnetohydrodynamic limit. At a distance $\tilde{r} = (1+S)^{-1}\ln S/\epsilon$, $S\,\frac{\partial v}{\partial \theta} = \epsilon$ and

the pressure gradient becomes important. At this point $-u = S(1+S)^{-1}$.

The boundary between these two cases is when $S \approx \epsilon^{1/2}$. In that case, when $\tilde{r} \approx \ln \epsilon^{-1/2}$ every term in (3.16) becomes of order ϵ. This justifies our earlier statement that $S \approx \epsilon^{1/2}$ was the critical value of S for the appearance of a slow flow region. It is important to note that as soon as there is a slow flow region, i.e., as soon as $S > \epsilon^{1/2}$, the normal component of the velocity takes up its limiting value $S/(1+S)$ at the back of the deceleration layer defined, for this case, as the place where $\partial v/\partial\theta = \epsilon/S$.

We calculate next the pressure gradient at the back of the deceleration layer, using (3.14). Now $\partial^2 p/\partial\theta^2 = -2$ at the shock, $\tilde{r} = 0$, since $p \sim \cos^2\theta$. Therefore, integrating:

$$-\frac{\partial^2 p}{\partial\theta^2} = 2 + \frac{\left[1 - e^{-2(1+S)\tilde{r}}\right]}{1+S} + 2S\,\frac{\partial B_\theta}{\partial\theta}\,\frac{\left[1 - e^{-(1+S)\tilde{r}}\right]}{1+S} \qquad (3.22)$$

As discussed earlier, we need only use this pressure gradient at the back of the layer where both exponentials are small. We define

$$k = -\left.\frac{\partial^2 p}{\partial\theta^2}\right|_{\substack{\theta = 0 \\ \tilde{r} = \infty}} = 2 + \frac{1}{1+S} + \frac{2S\,\dfrac{\partial B_\theta}{\partial\theta}}{1+S} \qquad (3.23)$$

The first of these terms represents the pressure gradient at the shock, the second is the centrifugal effect, and the third is the magnetohydrodynamic effect. For the dipole as shown in Fig. 2,

$$\left.\frac{\partial B_\theta}{\partial\theta}\right|_{\text{stag. pt.}} = \frac{2}{r_s} - 1 \qquad (3.24)$$

If the dipole happens to be at the center of curvature of the shock, $r_s = 1$. As anticipated, we see that the centrifugal effect is always weakened by the presence of a magnetic field, and that the magnetohydrodynamic effect can be of either sign depending on whether the field lines in the deceleration layer appear to diverge from a point ahead of or behind the center of curvature of the deceleration layer.

In order to find the remaining details of the deceleration layer, we substitute k for the pressure gradient in (3.16). As we have seen, this will not affect the solution near the front of the layer, (where $-\partial^2 p/\partial\theta^2 = 2$, not k), but is important at the back, where $\partial^2 p/\partial\theta^2$ is equal to k. (3.16) becomes

$$-u\frac{d}{d\tilde{r}}\left(\frac{\partial v}{\partial\theta}\right) + \left(\frac{\partial v}{\partial\theta}\right)^2 + S\frac{\partial v}{\partial\theta} - k\epsilon = 0 \qquad (3.25)$$

The equations (3.13) and (3.25) have been integrated by Lykoudis[3] on the incorrect assumption that k = 3, its aerodynamic value, obtained from (3.23) by setting S = 0. We have repeated the integration using (3.23) as appropriate. The correct stagnation point velocity gradient as a fraction of its non-magnetic value $(3\epsilon)^{1/2}$ is:

$$(3\epsilon)^{-1/2}\frac{\partial v}{\partial\theta} = -\frac{S}{(12\epsilon)^{1/2}} + \sqrt{\frac{S^2}{12\epsilon} + \frac{k}{3}} \qquad (3.26)$$

The stand-off distance $\Delta = (r_c - r_b)/r_c$ is:

$$\frac{\Delta}{\epsilon} = \frac{Q_0 - Q_1}{Q_0(1-Q_1)}\, F\left(1, \frac{Q_0}{Q_0-Q_1}, \frac{Q_0}{Q_0-Q_1} + 1 ; \frac{1-Q_0}{1-Q_1}\right) \qquad (3.27)$$

where F is the hypergeometric function, and

$$\begin{aligned} Q_0 &= \tfrac{1}{2} S\left[(1+a^2)^{1/2} - 1\right] \\ Q_1 &= \tfrac{1}{2} S\left[(1+a^2)^{1/2} + 1\right] \\ a^2 &= 4k\epsilon S^{-2} \end{aligned} \qquad (3.28)$$

The stagnation point velocity gradient ratio is plotted in Fig. 3a for the two-dimensional case and in Fig. 3b, from (A.3.26), for the axially symmetric case. The stand-off distance is plotted in Fig. 4a for the two-dimensional case and in Fig. 4b for the axially symmetric case. The differences from Lykoudis' calculation are not large when $S\epsilon^{-1/2}$ is small.

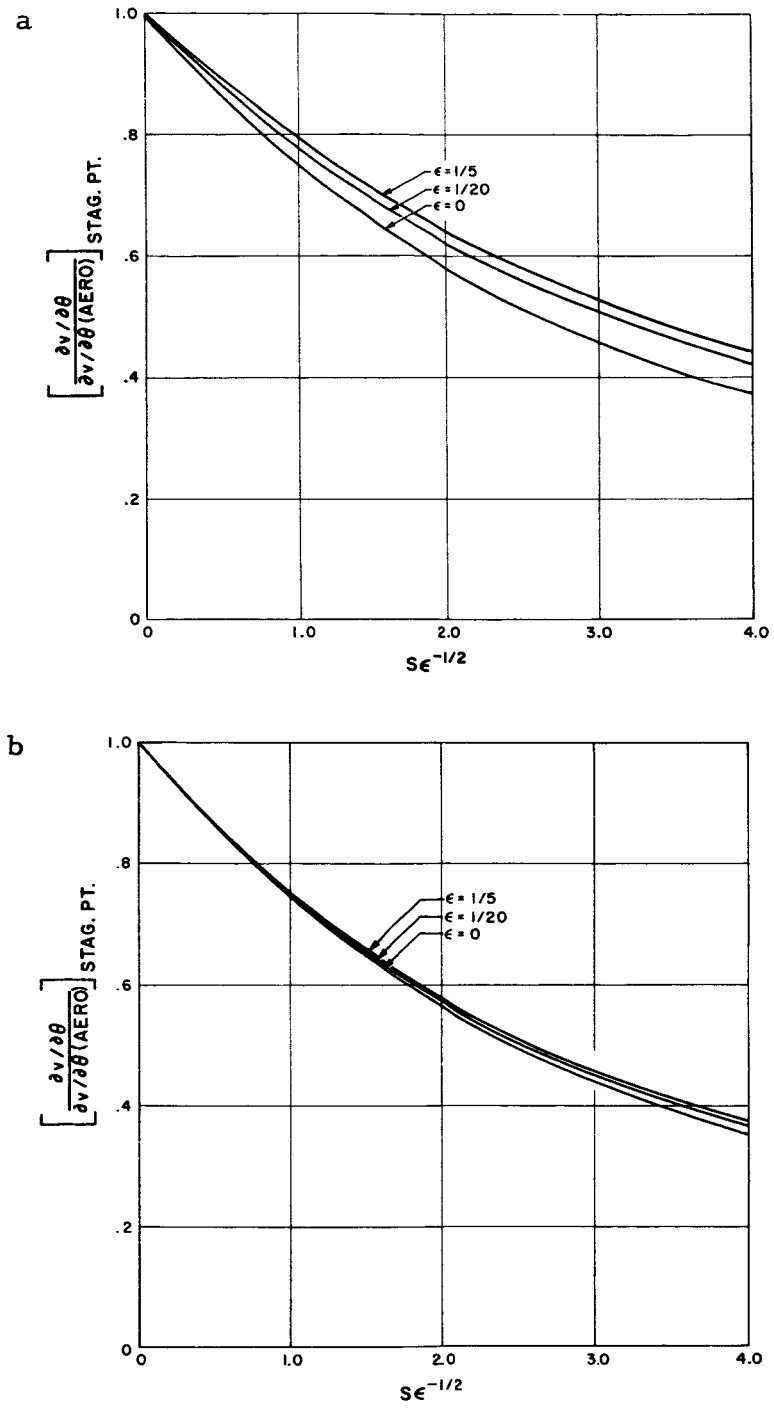

Fig. 3 Illustrates the reduction in the stagnation point velocity gradient effected by introducing a magnetic field. The calculation is reasonable only as far as $S\epsilon^{-1/2} \approx 1$. In this as in subsequent figures, a is the two-dimensional and b is the axially symmetric case.

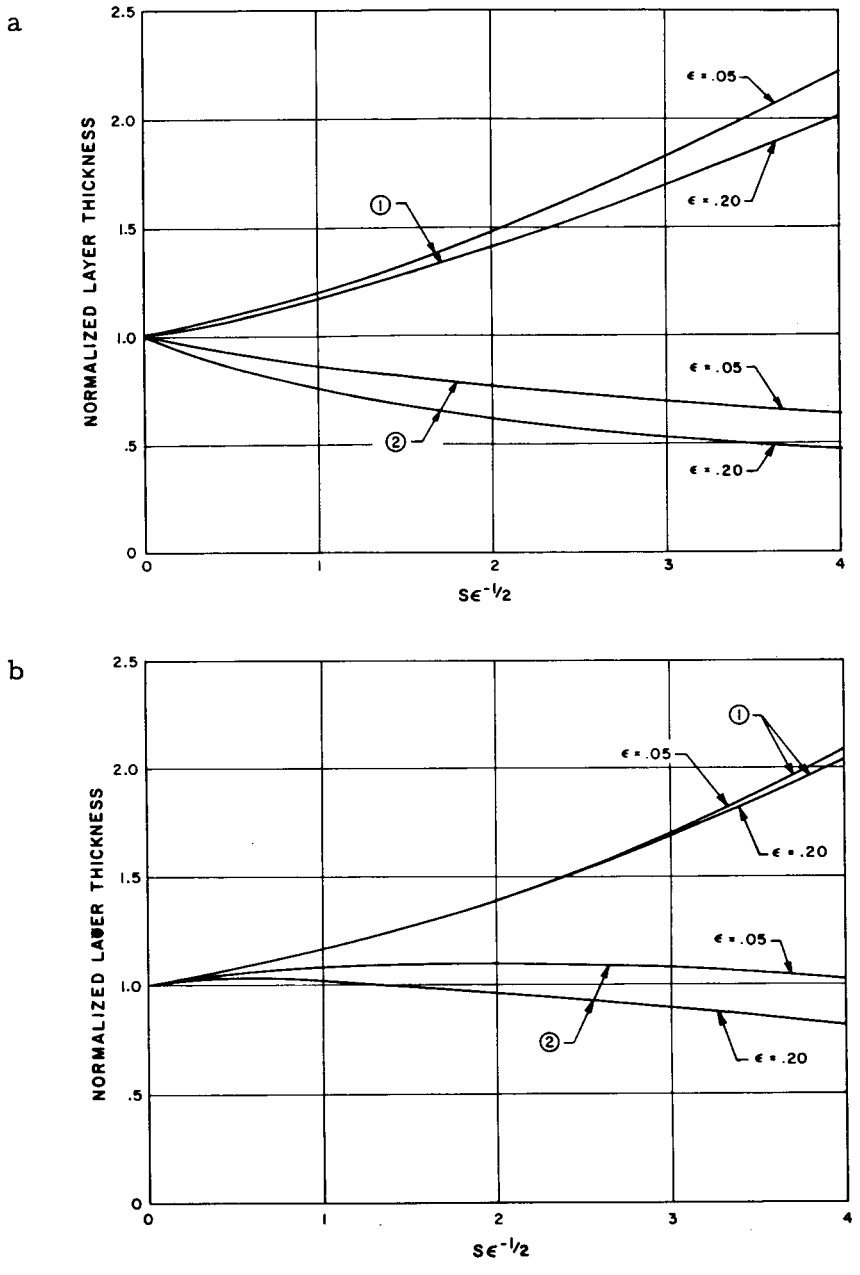

Fig. 4 Illustrates the increase in the shock stand-off distance effected by introducing a magnetic field. The calculation is reasonable only as far as $S\epsilon^{-1/2} \approx 1$. The lines marked (1) represent the entire stand-off distance. The lines marked (2) give the thickness of the deceleration layer defined as extending from the shock to the place where $-u = S(1+S)^{-1}$ in the two-dimensional case or $S^2(1+S)^{-2}$ in the axially symmetric case. All these lengths are normalized with respect to the appropriate aerodynamic shock layer thicknesses.

The lines on Fig. 3 marked $\epsilon = 0$ correspond exactly to Lykoudis' calculation in the sense that if $\epsilon = 0$, but $S\epsilon^{-1/2}$ is finite, S must be zero and hence k takes its aerodynamic value. Also shown in Fig. 4 are the thicknesses of the deceleration layer, defined as the region where $1 \geq -u \geq S(1 + S)^{-1}$ (for the two-dimensional case). The difference between these two lengths is the incipient slow flow region. All the lengths in Fig. 4 are normalized with respect to the aerodynamic stand-off distance, $\epsilon(1-3\epsilon)^{-1/2}\cosh^{-1}(3\epsilon)^{-1/2}$ in the two-dimensional case. It can be seen that with increasing $S\epsilon^{-1/2}$, the deceleration layer thickness does not change very much, while the total stand-off distance grows rapidly. This merely confirms our previous discussion in which, for large $S\epsilon^{-1/2}$ we divided the flow into a thin deceleration layer and a fat slow flow region. Fig. 4 therefore, illustrates the incipient growth of the slow flow region. It cannot, however, be used, as Lykoudis has used it, to determine the distance between the body and the shock when $S\epsilon^{-1/2} >$ about 1. The reasons for this are that the assumptions that went into (3.25) from which the numbers appearing in Fig. 4 were calculated, are violated as follows in the region $-u < S(1+S)^{-1}$:

a) The tangential velocity is reduced to the same order of magnitude as the radial velocity, so that, referring to (3.7), the current is no longer given by (3.8).

b) The fact that the velocity components are equal in order of magnitude implies that the scale of the problem is no longer compressed. Thus, the flow now extends over regions comparable in size in all directions with the body, and the pressure gradient can no longer be treated as constant.

c) The deceleration layer can no longer be assumed concentric with the body and the dipole.

To conclude this section, we point out that the type of analysis used here, in the magnetohydrodynamic as in the aerodynamic case, gives the stand-off distance of the shock in terms of the shock radius of curvature, but does not give the radius of curvature of the body. To establish the body radius of curvature we must consider the flow at greater distances from the stagnation streamline.

IV. SLOW FLOW REGION

We have seen that, when $S\epsilon^{-1/2} \gg 1$, there is a region between the deceleration layer and the body in which both velocity components are of order ϵu_∞. Since this velocity is strongly subsonic the enthalpy is effectively constant and from (3.2)

$$p = \rho \tag{4.1}$$

although these quantities will vary considerably through the region. We note that this isenthalpic motion may involve a considerable rise in the entropy. Since the flow is subsonic, we may neglect the convection of momentum and consider the flow to be governed by the remains of the momentum equation:

$$\nabla p = S\underset{\sim}{j} \times \underset{\sim}{B} \tag{4.2}$$

The neglect of the inertia term in (4.2) will result in infinite velocities; these should be interpreted as sonic. The equation of continuity is:

$$\nabla \cdot \rho \underset{\sim}{u} = 0 \tag{4.3}$$

These equations may be considered to have been non-dimensionalized just as before, with two exceptions. Both components of velocity are now non-dimensionalized with respect to ϵu_∞, and distances are referred simply to r_c. The current now involves contributions from both velocity components. We shall find it convenient to work in the polar coordinates (R, ϕ) fixed at the dipole and define the radial and tangential velocity components in these coordinates by means of a stream function ψ, non-dimensionalized with respect to $\rho_\infty u_\infty r_c$. The components are:

$$-\frac{1}{\rho R}\frac{\partial \psi}{\partial \phi}, \quad \frac{1}{\rho}\frac{\partial \psi}{\partial R} \tag{4.4}$$

We multiply (4.2) by $p = \rho$ and find

$$\frac{1}{2}\nabla p^2 = S(\rho \underset{\sim}{v} \times \underset{\sim}{B}) \times \underset{\sim}{B} \tag{4.5}$$

When we substitute from (4.4) in (4.5) we find two linear equations (the components of 4.5) for the two unknowns p^2 and ψ. The field components are

$$\underset{\sim}{B} = \left(\frac{r_s}{R}\right)^2 \cos\phi, \left(\frac{r_s}{R}\right)^2 \sin\phi \tag{4.6}$$

and the components of (4.5) are:

$$\frac{1}{2}\frac{\partial p^2}{\partial R} = S\left(\frac{r_s}{R}\right)^4 \sin\phi\left[\cos\phi\frac{\partial\psi}{\partial R} + \frac{\sin\phi}{R}\frac{\partial\psi}{\partial\phi}\right] \tag{4.7}$$

$$\frac{1}{2R}\frac{\partial p^2}{\partial\phi} = -S\left(\frac{r_s}{R}\right)^4 \cos\phi\left[\cos\phi\frac{\partial\psi}{\partial R} + \frac{\sin\phi}{R}\frac{\partial\psi}{\partial\phi}\right] \tag{4.8}$$

Multiply (4.7) by $\cos\phi$, (4.8) by $\sin\phi$ and add:

$$\left[\cos\phi\frac{\partial}{\partial R} + \frac{\sin\phi}{R}\frac{\partial}{\partial\phi}\right] p^2 = 0 \tag{4.9}$$

This equation implies that p is a function only of

$$\eta = \frac{r_s^2 \sin\phi}{R} \tag{4.10}$$

This result states only, as might have been seen at once from (4.2), that the pressure has a constant value on any field line. Now multiply (4.7) by $\sin\phi$, (4.8) by $\cos\phi$ and subtract:

$$\left[\sin\phi\frac{\partial}{\partial R} - \frac{\cos\phi}{R}\frac{\partial}{\partial\phi}\right]\frac{1}{2}p^2 = S\left(\frac{r_s}{R}\right)^4\left[\cos\phi\frac{\partial\psi}{\partial R} + \frac{\sin\phi}{R}\frac{\partial\psi}{\partial\phi}\right] \tag{4.11}$$

Using the fact that $p = p(\eta)$, the left hand side of this is equivalent to:

$-\frac{1}{2}\left(\frac{r_s}{R}\right)^2 \frac{dp^2}{d\eta}$ so that

$$-\frac{1}{2}\frac{dp^2}{d\eta} = S\left(\frac{r_s}{R}\right)^2 \left[\cos\phi \frac{\partial\psi}{\partial R} + \frac{\sin\phi}{R} \frac{\partial\psi}{\partial\phi}\right] \tag{4.12}$$

In view of the fact that $dp^2/d\eta$, like p, is a function of η alone, we can find solutions of (4.12) of the form

$$\psi = -\frac{1}{2S} \frac{dp^2}{d\eta} G(R,\phi) \tag{4.13}$$

G satisfies the equation

$$\left(\frac{r_s}{R}\right)^2 \left[\cos\phi \frac{\partial G}{\partial R} + \frac{\sin\phi}{R} \frac{\partial G}{\partial\phi}\right] = 1 \tag{4.14}$$

A particular solution of this equation may be found in the form

$$G = \frac{R^3}{r_s^2} g(\phi) \tag{4.15}$$

where g satisfies

$$\sin\phi\, g' + 3\cos\phi\, g = 1 \tag{4.16}$$

This has only one solution finite at $\phi = 0$ and it is:

$$g = \frac{\phi - \sin\phi\cos\phi}{2\sin^3\phi} \tag{4.17}$$

In addition, any function $h(\eta)$ satisfies the homogeneous part of (4.14) so that the general solution of the problem is

$$\psi(R,\phi) = -\frac{1}{2S} \frac{dp^2}{d\eta}\left[\frac{R^3}{r_s^2}\left\{\frac{\phi - \sin\phi\cos\phi}{2\sin^3\phi}\right\} + h(\eta)\right] \tag{4.18}$$

This equation tells us everything we need to know about the slow flow region. We notice in particular that ψ vanishes on three separate lines: First, on the stagnation streamline since (by symmetry) $dp/d\eta$ vanishes; Second on the body where the quantity in square braces vanishes. Since $h(\eta)$ is arbitrary any body can be described. Finally, ψ vanishes on the two symmetrically placed field lines for which p vanishes. In order to illustrate these remarks, let us consider a cylindrical body R = a. We find:

$$h\left(\frac{r_s^2 \sin\phi}{a}\right) + \frac{a^3}{r_s^2}\left\{\frac{\phi - \sin\phi\cos\phi}{2\sin^3\phi}\right\} = 0 \qquad (4.19)$$

$$h(\eta) = \frac{r_s^4}{2\eta^3}\left[\frac{\eta a}{r_s^4}\sqrt{r_s^4 - \eta^2 a^2} - \sin^{-1}\left(\frac{\eta a}{r_s^2}\right)\right] \qquad (4.20)$$

giving, finally

$$\psi(R,\phi) = -\frac{1}{2S}\frac{dp^2}{d\eta}\frac{R^3}{r_s^2}\left[\frac{\phi - \sin^{-1}\left(\frac{a}{R}\sin\phi\right) - \sin\phi\cos\phi + \left(\frac{a}{R}\sin\phi\right)\sqrt{1 - \frac{a^2\sin^2\phi}{R^2}}}{2\sin^3\phi}\right] \qquad (4.21)$$

A number of interesting conclusions may be drawn from this analysis. First, given the pressure at any point at the back of the deceleration layer, that pressure obtains for the whole field line passing through the given point. The density is similarly determined. Secondly, if the pressure gradient along the back of the deceleration layer is also given, we can find the component of this gradient across the field lines, and hence, from (4.21), the mass flow out of the shock layer. In order to give a more concrete idea of the type of flow represented by (4.21) we have in Fig. 5 drawn the streamlines in the slow flow region for a highly idealized (and somewhat artificial) pressure distribution and shock shape. We assume the shock to be semicircular and centered at the dipole; thus $R = r_s = 1$ is the equation of the shock. We assume the pressure to be given by $p = \cos^2\phi$ on the shock. Through the flow field, then, p is given by

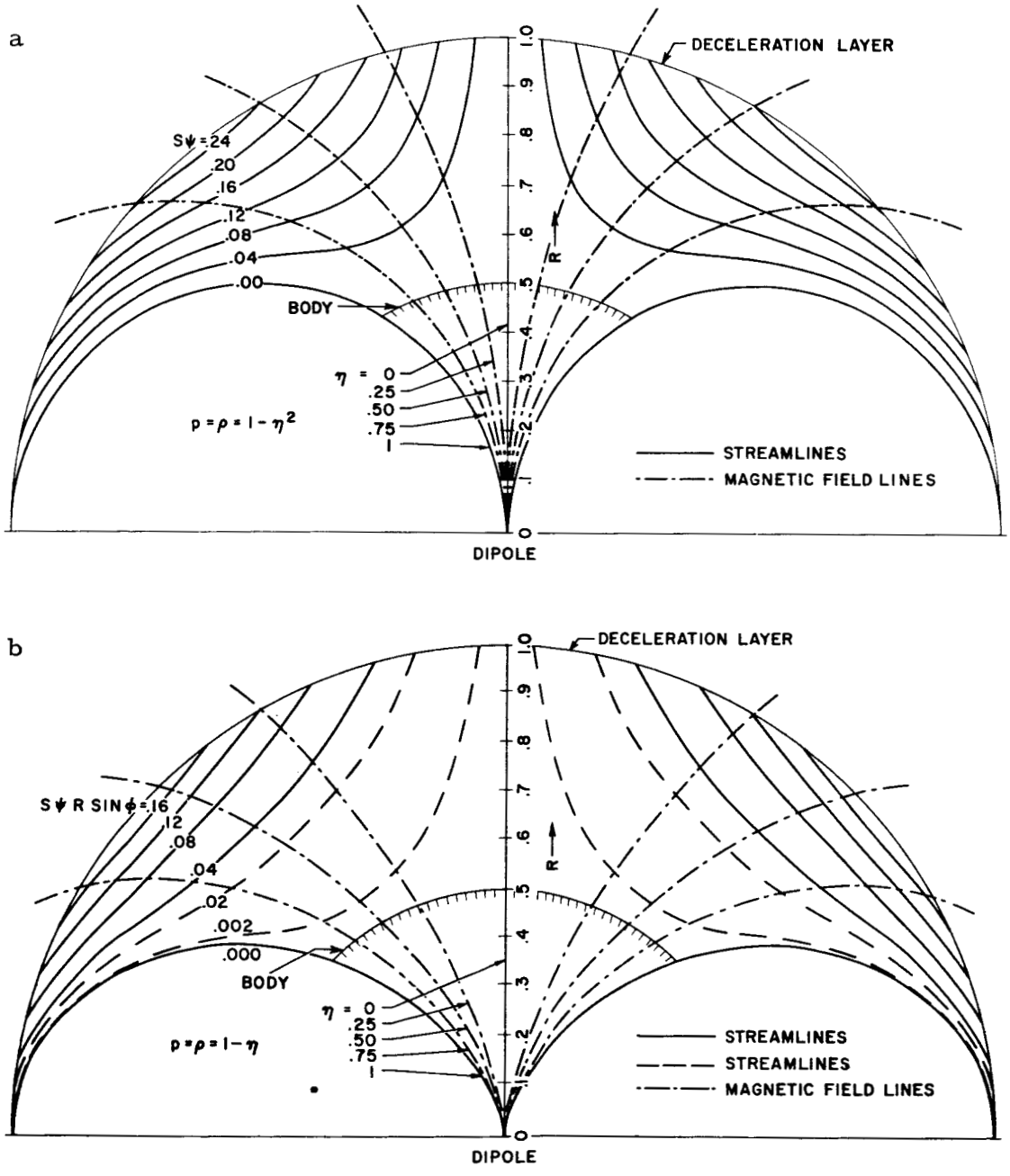

Fig. 5 As explained in the text, this figure is to be regarded as illustrating a typical flow in the slow flow region rather than representing a physically realistic solution. The streamtubes indicated by solid lines carry equal mass fluxes. Two additional streamlines are shown in b. In both cases the limiting streamline $\psi = 0$ is also a field line. The pressure and density are constant on field lines in the slow flow region. The formulae connecting the pressure and density with η, the field line parameter, are shown.

$$p = p(\eta) = 1 - \eta^2 \tag{4.22}$$

We also assume the body to be of radius $a = \frac{1}{2}$. The stream function is, therefore, given by:

$$S\psi = \left(\frac{R^2}{\sin^2\phi} - 1\right)\left[\phi - \sin^{-1}\left(\frac{\sin\phi}{2R}\right) - \sin\phi\cos\phi + \frac{\sin\phi}{2R}\sqrt{1 - \frac{\sin^2\phi}{4R^2}}\right] \tag{4.23}$$

In view of the artificial construction of this picture, no significance whatever should be attached to the fact that streamlines entering the slow flow region near the axis appear to leave it further round by going back into the deceleration layer. This is not regarded as a likely physical situation. What is important to note from this figure, however, is the small role which the body plays in determining the whole flow. In fact it is fairly clear that the body could be reduced in size without substantially changing the flow. Ultimately we can reach the situation where there is no body in the flow at all; this corresponds to $h(\eta) \equiv 0$. Finally it should be remembered that the part of the cylinder sketched in Fig. 5 is in contact with a hot flow, but the gas density reaches zero on the limiting field lines. Beyond these lines the body could be of any shape without affecting the flow at all. Put another way, Fig. 5 illustrates the manner in which the magnetic interaction can remove large areas of the body from any contact with the flow. This is clearly a result of the highest importance in considering the heat transfer; at the same time the result is not obtainable from a consideration of the flow only in the vicinity of the stagnation streamline.

V. MATCHING IN THE VICINITY OF THE STAGNATION STREAMLINE

We can reach useful conclusions concerning the relationships that connect S, r_s and r_b by using the results of Section III and the results of Section IV specialized to the stagnation streamline $\theta = \phi = 0$. At the back of the deceleration layer the pressure is given for small values of θ from (3.23) and (3.24) by:

$$p \approx 1 - \frac{1}{2} k\theta^2 \tag{5.1}$$

For small θ and ϕ, the field-line parameter η defined in (4.10) is

$$\eta \approx \frac{r_s^2 \phi}{R} \approx \frac{r_s^2 r\theta}{R^2} \tag{5.2}$$

and on the shock $R = r_s$, $r = 1$. Since, in the slow flow region, p is a function of η alone, we can combine (5.1) and (5.2) to give

$$p \approx 1 - \frac{1}{2} k\eta^2 \tag{5.3}$$

which is valid for small η, (and therefore for small ϕ), but for any r between the shock and the body. Next, we specialize the general solution for the stream function in the slow flow region (4.18) to the stagnation streamline. This gives us

$$\psi \approx \frac{r\theta k}{3S} \left[R + \frac{3 r_s^2 h(o)}{R^2} \right] \tag{5.4}$$

From this relation we can find the flow near $\theta = 0$ all the way from the shock to the body. In particular, at the shock we can calculate the radial velocity

$$u = -\frac{1}{\rho r_s} \frac{\partial \psi}{\partial \phi} = \frac{-\partial \psi}{\partial \theta} \Bigg|_{\substack{r = 1 \\ \theta = 0}} \tag{5.5}$$

However, this radial velocity has already been calculated in (3.21). It is just the residual radial velocity at the back of the deceleration layer. Thus we find the important matching condition

$$\frac{S}{1+S} = \frac{k}{S}\left[\frac{1}{3}r_s + h(o)\right] \tag{5.6}$$

which yields:

$$S^2 - \left(\frac{4}{3}S + r_s\right)\left(1 + \frac{3h(o)}{r_s}\right) = 0 \tag{5.7}$$

To find h(o), we recall that the body is given when $\psi = 0$ as a result of the vanishing of the last bracket in (5.4). Thus:

$$r_b + 3\left(\frac{r_s}{r_b}\right)^2 h(o) = 0 \tag{5.8}$$

Eliminating h(o) between (5.7) and (5.8) gives:

$$S^2 - \left(\frac{4}{3}S + r_s\right)\left[1 - \left(\frac{r_b}{r_s}\right)^3\right] = 0 \tag{5.9}$$

This is the sought after relation between S, r_s and r_b. From it we can make a number of deductions, the most important of which is the following: In a given flight situation (i.e. $\rho_\infty u_\infty$ and ϵ given, as well as the magnetic moment of the dipole and its location relative to the body), (5.9) does not give unique values for the quantities appearing in it. We recall that r_b and r_s are non-dimensionalized with respect to r_c, and that r_c is also the length appearing in the definition of S. Suppose some value of r_c is given; then from the geometry we can calculate r_b. However, S is proportional to B_o^2, which in turn is proportional to the inverse fourth or sixth (depending on the dimensionality) power of r_s. (5.9) is then an equation for r_s. But this procedure will be valid for any r_c, and there is no way of knowing which is correct. One solution to this difficulty is by making Bush's ad hoc

assumption $r_s = 1$, implying that the dipole is at the center of curvature of the shock. (5.9) can then be interpreted as an equation for r_c. As indicated in Section II, we prefer to deal with this ambiguity by means of a construction of the flow away from the stagnation streamline; while this approach is undoubtedly superior from the theoretical point of view, it is quite difficult for various reasons. The flow picture that we shall construct is therefore not entirely satisfactory. In the end, we shall see, however, that the results of our calculations do not disagree strongly with the assumption $r_s = 1$. We believe that this fact lends greater credibility to Bush's calculations, and at the same time tends to support the flow model away from the stagnation region which we shall adopt.

Returning for the moment to (5.9), we measure the stand-off distance by means of a non-dimensional distance Δ given by:

$$\Delta = \frac{r_s}{r_b} - 1 \tag{5.10}$$

Hence, in terms of S and r_s,

$$\Delta = \left[1 - \frac{S^2}{\frac{4}{3} S + r_s} \right]^{-1/3} - 1 \tag{5.11}$$

The stand-off distances calculated in this way are not directly comparable to the aerodynamic stand-off distance. For the aerodynamic stand-off distance is a quantity of order ϵ while Δ in (5.11) is of order unity. This is a result of the slow flow region having comparable dimensions parallel and perpendicular to the flow. These remarks also explain why, if we put $S = 0$ in (5.11) we recover $\Delta = 0$.

There are values of S and r_s such that $\Delta \to \infty$. They satisfy the relation

$$S^2 - \frac{4}{3} S - r_s = 0 \tag{5.12}$$

These values are of particular interest to us. They do not correspond to an infinite distance from the shock to the dipole, but rather to a zero dis-

tance between the body and the dipole $r_b = 0$. Thus, they correspond to what we refer to as the fully magnetohydrodynamic case. The region on the body in contact with the flow shrinks to a point and the entire drag generated by the flow field is felt by the magnet.

We can compare our analytical calculations (for $\epsilon \ll 1$) up to this point with Bush's numerical calculations for $\epsilon = 1/11$ by setting $r_s = 1$ in the axially symmetric analogue of (5.11), that is, in (A.5.11). When the interaction parameters are modified to allow for differences in notation, the agreement is quite good. In particular, for the axisymmetric case, Bush finds $\Delta = \infty$ for $S \approx 1.53$. This compares with our value $\Delta = \infty$ for $S = 1.90$ from (A.5.12) with $r_s = 1$. The difference can probably be attributed to finite ϵ effects.

VI. DECELERATION LAYER ANALYSIS AWAY FROM THE STAGNATION STREAMLINE

To study the behavior of the deceleration layer away from the stagnation streamline we have to resort to approximate methods in the absence of analytic solutions. Since we do not know a priori the shape of the layer we have to introduce an arbitrary system of coordinates fixed in the layer. This system is shown in Fig. 6. n and s are coordinates perpendicular and parallel to the layer. The position of the layer itself is referred to Cartesian coordinates fixed at the center of curvature of the normal part of the layer. Thus, it is given parametrically in terms of the arc length s by:

$$\left.\begin{aligned} x &= x_L(s) \\ y &= y_L(s) \end{aligned}\right\} \tag{6.1}$$

the subscript referring to the layer. Since s is arc length we have

$$\dot{x}_L^2 + \dot{y}_L^2 = 1 \tag{6.2}$$

where dots denote differentiation with respect to s. Using (as before) r_c as the unit of length, x_L and y_L are given for small s by:

$$\left.\begin{aligned} x_L &= 1 - \frac{1}{2} s^2 \ldots. \\ y_L &= s - \frac{1}{6} s^3 \ldots. \end{aligned}\right\} \tag{6.3}$$

u and v are the components of velocity in the n and s directions. Since the thickness of the layer is on the order of ϵr_c we introduce a coordinate $\tilde{n}$ such that $\tilde{n} = 0$ is at the shock and

$$\frac{\partial}{\partial \tilde{n}} = -\frac{1}{\epsilon} \frac{\partial}{\partial n} \tag{6.4}$$

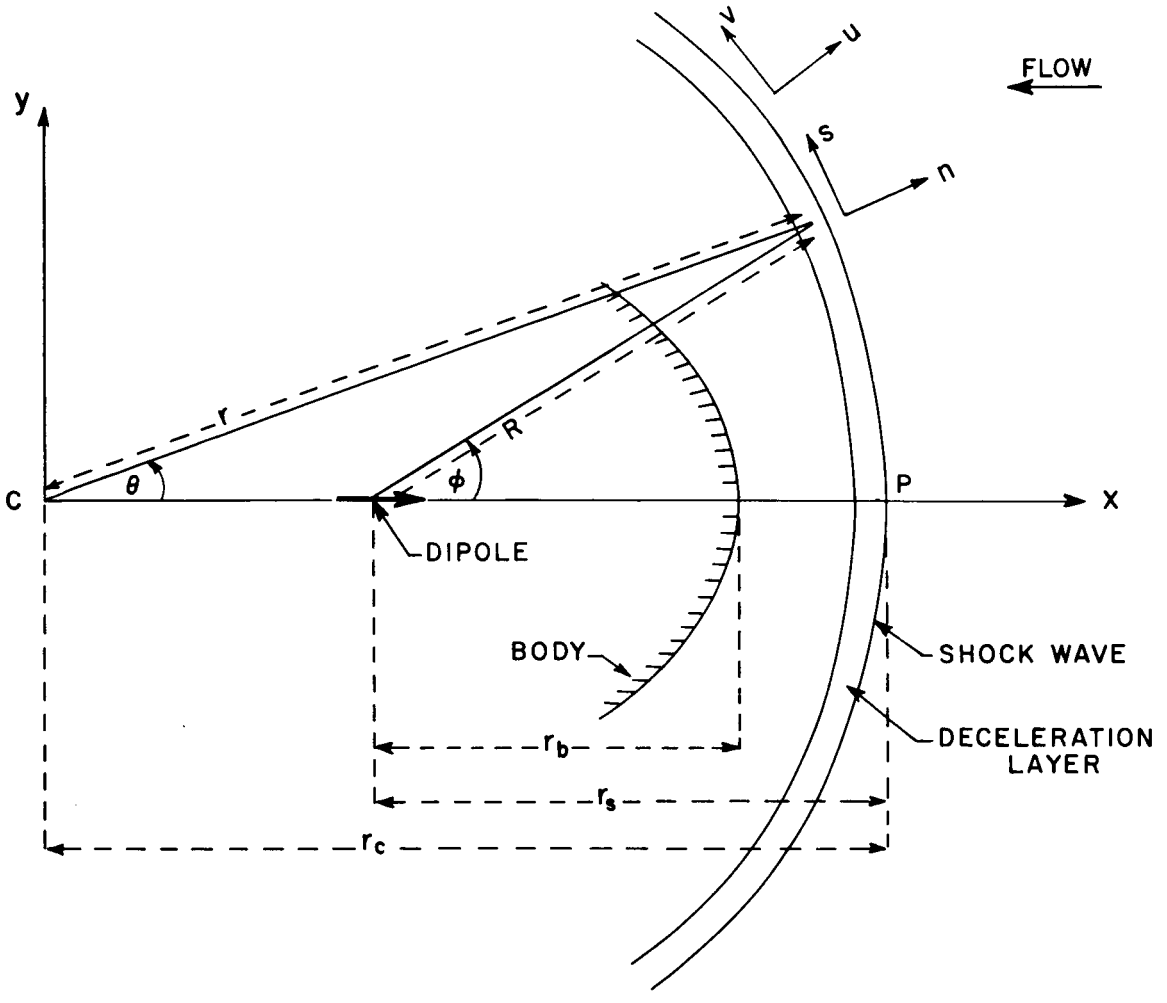

Fig. 6 Illustrates the coordinate system used in Section VI of the text. C is the center of curvature of the deceleration layer at the point P. The components (u, v) of the velocity are, respectively, in the n and s directions. In the text, the length r_c is taken to be unity.

Thus, $\tilde{n}$ is a generalization of the coordinate $\tilde{r}$ used in Section III. The continuity equation corresponding to (3.4) is

$$\frac{\partial}{\partial \tilde{n}} (\rho u) - \frac{\partial}{\partial s} (\rho v) = 0 \tag{6.5}$$

where, as in Section III, u and v are non-dimensionalized with respect to ϵu_∞ and u_∞ respectively. The current is effectively given by

$$j = -vB_n \tag{6.6}$$

where B_n is the component of the magnetic field normal to the layer. This expression is valid until B_n is comparable with ϵB_s, where B_s is the component of the magnetic field parallel to the layer. At this point, as we will see, the current no longer affects the dynamics of the layer appreciably and can therefore be neglected. B_s and B_n may be regarded as functions of s only, and are given by:

$$\left.\begin{aligned} B_s &= \dot{x}_L B_x + \dot{y}_L B_y \\ B_n &= \dot{y}_L B_x - \dot{x}_L B_y \end{aligned}\right\} \tag{6.7}$$

where B_x and B_y, the x and y components of the magnetic field, are given by

$$\left.\begin{aligned} B_x &= \left(\frac{r_s}{R}\right)^2 \cos 2\phi \\ B_y &= \left(\frac{r_s}{R}\right)^2 \sin 2\phi \end{aligned}\right\} \tag{6.8}$$

The normal momentum equation becomes

$$\kappa \rho v^2 + \frac{\partial p}{\partial \tilde{n}} + S v B_n B_s = 0 \tag{6.9}$$

which is a generalization of (3.9). κ, the curvature of the layer, is a function only of s, and is given by

$$\kappa = \dot{x}_L \ddot{y}_L - \dot{y}_L \ddot{x}_L \tag{6.10}$$

The s-momentum equation becomes

$$\rho u \frac{\partial v}{\partial \tilde{n}} - \rho v \frac{\partial v}{\partial s} - S v B_n^2 = 0 \tag{6.11}$$

which is a generalization of (3.15). Finally the energy equation is just the same as (3.2), that is

$$p = \rho(1-v^2) \tag{6.12}$$

At the shock, $\tilde{n} = 0$, we have the following boundary conditions:

$$\rho = 1;\ p = \dot{y}_L^2;\ u = -\dot{y}_L;\ v = -\dot{x}_L \tag{6.13}$$

As indicated earlier, we lack general solutions to these equations. Consequently, we resort to a momentum integral method somewhat analogous to that used in boundary layer theory.[7] We introduce the quantities

$$I(s) = \int v d\tilde{n} \qquad M(s) = \int \rho v d\tilde{n} \qquad P(s) = \int \rho v^2 d\tilde{n} \tag{6.14}$$

These quantities measure, respectively, the current, mass flux and momentum flux in the deceleration layer. The integrals are carried from the shock $\tilde{n} = 0$ to the effective back of the layer. On integrating (6.9) across the layer we find

$$\kappa P + p_M - \dot{y}^2 + S B_n B_s I = 0 \tag{6.15}$$

where $p_M(s)$ is the pressure at the back of the deceleration layer. The subscript indicates that we will use this quantity to match with our solution for the flow in the slow flow region. (6.15) is, of course, an equation in which all the quantities occurring are functions only of s. Integrating (6.11) through the layer gives:

$$\int \rho u \frac{\partial v}{\partial \tilde{n}} \, d\tilde{n} - \int \rho v \frac{\partial v}{\partial s} \, d\tilde{n} - SB_n{}^2 I = 0 \tag{6.16}$$

On integrating the first term by parts, using the continuity equation (6.5), and combining with the second term we find

$$[\rho uv] - \int \frac{\partial}{\partial s} (\rho v^2) \, d\tilde{n} - SB_n{}^2 I = 0 \tag{6.17}$$

We can evaluate ρuv at the shock using (6.13). At the back of the layer it is effectively zero since v is reduced to the order of ϵ at that point. Thus:

$$\dot{x}_L \dot{y}_L + \dot{P} + SB_n{}^2 I = 0 \tag{6.18}$$

Rather than evaluate the normal component of velocity at the back of the layer, it is convenient to introduce a stream function appropriate to the layer defined by:

$$\rho u = - \frac{\partial \psi}{\partial s} \qquad \rho v = - \frac{\partial \psi}{\partial \tilde{n}} \tag{6.19}$$

Noting that $\psi = y_L$ at the shock, integration of the second equation (6.19) gives

$$M = y_L - \psi_M \tag{6.20}$$

where ψ_M is the stream function at the back of the shock layer. ψ_M and p_M are the two quantities we use to relate the deceleration layer to the slow flow region.

An interesting observation to make on (6.15) and (6.18) is that if S = 0, corresponding to the aerodynamic case, we can eliminate P directly and find

$$p_M = \dot{y}^2 + \kappa \int_0^s \dot{x}_L \dot{y}_L ds \tag{6.21}$$

which is just the Busemann relation[8] for the pressure in Newtonian shock

layers. When the magnetic interaction is present, no such simple result is available to us. We have to assume profiles for v and ρ through the layer in terms of a shape parameter $\delta(s)$ of some kind, so that I, M and P can all be expressed as functions of $\delta(s)$. The equations (6.2), (6.10), (6.15), (6.18) and (6.19) then reduce to a system of five ordinary differential equations for the six unknowns x_L, y_L, κ, δ, ψ_M and p_M. To complete the set we need to introduce one further relation, and that is the slow flow solution (4.18). Along the deceleration layer we have

$$\frac{d\eta}{ds} = B_n \tag{6.22}$$

so that (4.18) becomes:

$$\psi_M = -\frac{p_M}{SB_n}\frac{dp_M}{ds}\left[\frac{r_s^4}{2\eta^3}(\phi - \sin\phi\cos\phi) + h(\eta)\right] \tag{6.23}$$

The equations described above can be used to solve two fundamentally different problems. The first of these, which we call the direct problem (by analogy to a somewhat similar aerodynamic problem) is that in which the body shape and the dipole location relative to the body are given. It is required to find the shape of the shock wave and the deceleration layer. The second problem, which we call the inverse problem is that in which the shape of the shock wave and deceleration layer are given, and also the location of the dipole relative to the shock wave. It is required to find the body shape. We shall give numerical examples of both these types of problems in the next section, but before proceeding to these calculations we must consider again our model (Section II) of the flow in the region away from the stagnation streamline. We have seen how to calculate along the deceleration layer, and we have seen how to join to the deceleration layer a consistent slow flow region. How far can we take this process?

As we proceed along the deceleration layer p_M falls. Eventually it will reach zero at which point the deceleration layer is fully supported by the centrifugal and j x B forces. Clearly, this point is a natural limit to the validity of our calculation. Another such limit can be found by considering the component of magnetic field normal to the deceleration layer. In

all reasonable configurations this field component must drop and it too will eventually reach zero at which point the deceleration layer is parallel to the magnetic field. We assume that these two points (i. e. the points where p_M and B_n vanish) coincide.

In justification of this model, suppose first that p_M reaches zero while B_n is finite. (6.23) shows that at this point $\psi_M = 0$, that is the stagnation streamline reaches the deceleration layer at this point. This implies that all the slow flow region is exhausted by being forced back into the deceleration layer. By the definition of the deceleration layer this implies that the slow flow is accelerated at least to sonic velocity in some region near the back of the deceleration layer. But the j x B force would oppose this acceleration and therefore, if it exists, it must be due to the pressure gradient. But in Section III we saw that as long as $S\epsilon^{-1/2} \gg 1$, the j x B force is always greater than the pressure gradient. The argument given there is directly applicable to our case as long as B_n remains of order unity. If B_n is of order $\epsilon^{1/4}$, however, the effective interaction parameter makes $S\epsilon^{-1/2} \sim 1$ in which case the pressure gradient does become important. But, on our assumption that $\epsilon^{1/4}$ is small, this implies that B_n is small which is contrary to our hypothesis. Thus we reject situations in which p_M goes to zero before B_n. Note that the argument given above about slow flow gas re-entering the deceleration layer makes part of Fig. 5 unacceptable. The weakest link in the above argument is the assumption $\epsilon^{1/4} \ll 1$. We shall discuss the implications of finite ϵ in Section VIII.

Returning to our model, suppose on the other hand that B_n goes to zero before p_M. From (6.23) we see that if ψ_M is to remain finite (which is physically essential) either dp_M/ds must vanish or the quantity in braces must vanish. If dp_M/ds vanishes for finite p_M, p_M goes through a minimum and starts to increase again. This seems to be unrealistic. The quantity in braces, on the other hand, vanishes at the body and cannot vanish twice on the same field line.

We are, therefore, led (by reductio ad absurdum) to suppose that p_M and B_n vanish simultaneously and that ψ_M is finite at that point. What are the consequences of this model? While the numerical answers to this question will be given in the next section, it will be useful to anticipate

certain results. At the point where p_M and B_n vanish, the slow flow velocity becomes infinite. This infinity must be regarded as meaning sonic. However, formally speaking, the area required to pass a finite mass at infinite velocity is zero provided the density is not zero, a condition which is certainly fulfilled for isothermal flow which expands by a factor $e^{1/2}$ in going from stagnation to sonic conditions. Therefore, all the slow flow gas must be immediately behind the point where p_M and B_n go to zero and the field line through this point delimits the flow in the sense that it must coincide with $\psi = 0$. This point, which has practical importance will be reviewed in Section VIII in the light of a more realistic view of the gas properties.

VII. RESULTS OF NUMERICAL CALCULATIONS

We consider first the choice of profiles to be used in calculating I, M and P. We introduce the following quantities: $\delta(s)$ is an effective thickness of the deceleration layer. ξ, defined by

$$\xi = \frac{\tilde{n}}{\delta} \tag{7.1}$$

varies from zero at the shock to unity at the back of the layer. We let

$$\frac{v}{-\dot{x}_L} = f_1(\xi) \tag{7.2}$$

$$\rho = f_2(\xi) \tag{7.3}$$

Thus, at the shock we have $f_1(o) = f_2(o) = 1$. At the back of the deceleration layer v is of order ϵ, and thus may be taken to be zero, that is $f_1(1) = 0$, and, from the energy equation (6.12), $f_2(1) = p_M$. These boundary conditions suffice to define linear profiles:

$$f_1(\xi) = 1 - \xi \tag{7.4}$$

$$f_2(\xi) = 1 - (1-p_M)\xi \tag{7.5}$$

With these profiles we readily calculate:

$$I(s) = -\dot{x}_L \delta \int_o^1 f_1(\xi) d\xi = -\frac{1}{2} \dot{x}_L \delta \tag{7.6}$$

$$M(s) = -\dot{x}_L \delta \int_o^1 f_1 f_2 \, d\xi = -\frac{1}{6} \dot{x}_L \delta (2 + p_M) \tag{7.7}$$

$$P(s) = \dot{x}_L{}^2 \delta \int_o^1 f_1{}^2 f_2 \, d\xi = \frac{1}{12} \dot{x}_L{}^2 \delta (3 + p_M) \tag{7.8}$$

Before we can use these for integration we must examine their behavior for small s. Since the linear profiles do not agree with the exponential profiles calculated in Section III, we may expect that the starting conditions developed in Section V will have to be modified. Now for small s, from (6.3), $\dot{x}_L \approx -s$, $\dot{y}_L \approx 1 - \frac{1}{2}s^2$. Thus, writing $\delta_o = \delta(o)$, (6.18) yields:

$$\delta_o = \frac{2}{S + 4/3} \tag{7.9}$$

Similarly, for small s, (6.15) yields:

$$k = 2 + \delta_o \left[\frac{2}{3} + S\left(\frac{2}{r_s} - 1 \right) \right] \tag{7.10}$$

Substitution from (7.9) gives

$$k = 2 + \frac{4/3}{S + 4/3} + \frac{2S}{S + 4/3}\left(\frac{2}{r_s} - 1 \right) \tag{7.11}$$

which must be regarded as an approximation to (3.23). It is seen that while there are numerical differences between these formulae, the general behavior is identical. From (6.20) we find, for small s,

$$\psi_M \approx \frac{S + 1/3}{S + 4/3}\, s \tag{7.12}$$

and, from (6.23)

$$S(S + 1/3) - \frac{4}{3}(S + r_s)\left[1 - \left(\frac{r_b}{r_s} \right)^3 \right] = 0 \tag{7.13}$$

where we have also used (5.8). This approximate equation replaces the exact result (5.9). The two equations are plotted for comparison in Fig. 7 where it is seen that no substantial errors are involved. Presumably, more involved profiles would reduce the discrepancies shown in Fig. 7, but the increased complexity involved would produce only a small increase in accuracy, and add nothing to our general understanding of the problem.

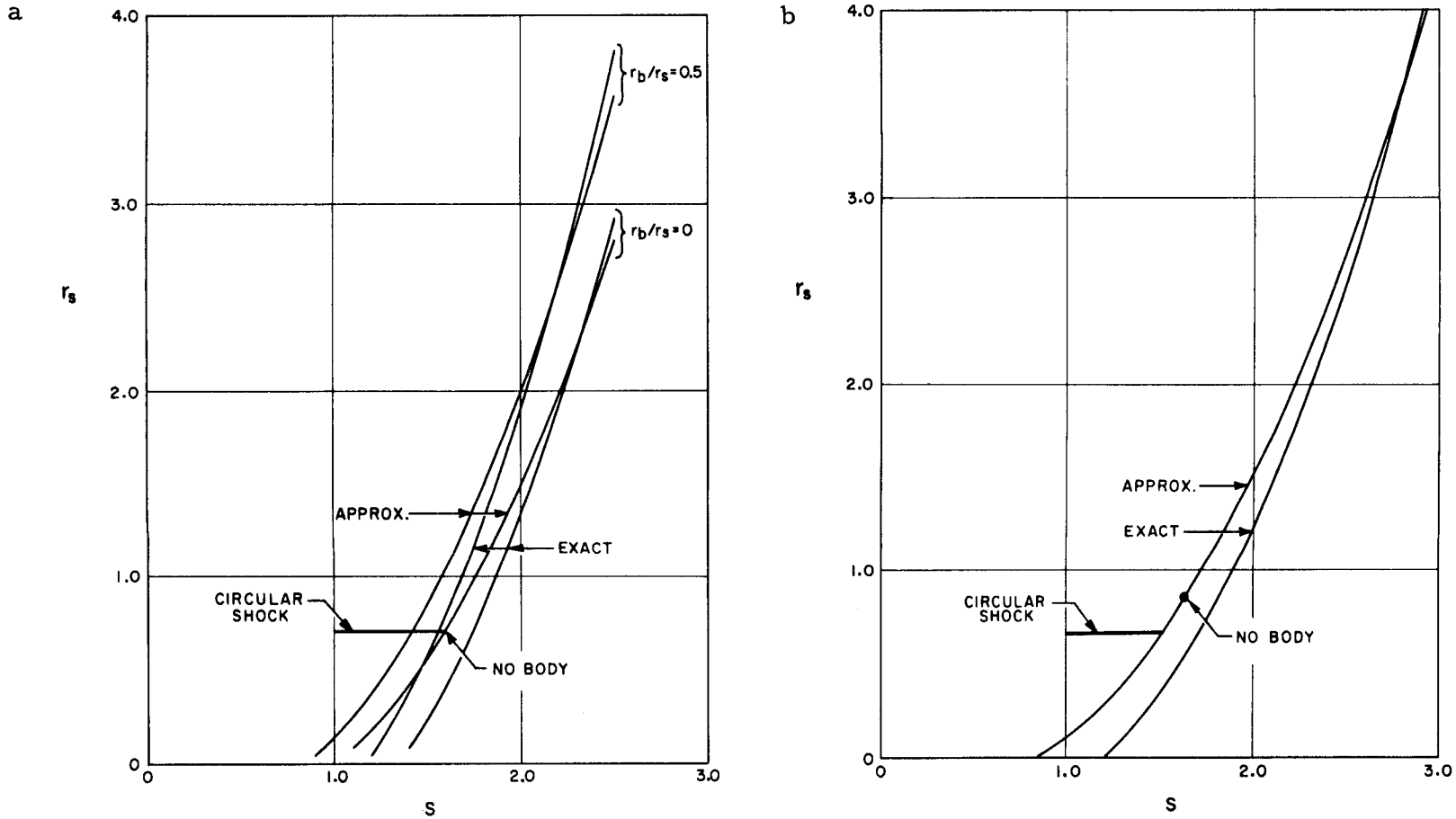

Fig. 7 Illustrates the exact and approximate relations connecting S, r_s and r_b. a compares (5.9) and (7.13) for two values of the ratio r_b/r_s. b compares (A.5.9) and (A.7.13). For this case the dependence on r_b/r_s is so weak that the curves shown can be taken to refer equally to the cases $r_b/r_s = 0$ or 1/2. Also shown are lines marked "circular shock" and points marked "no body." Detailed calculations of these cases are discussed in Section VII.

We have chosen two problems for detailed numerical treatment. Problem A, characteristic of the inverse problem, consists of finding the shapes of the bodies that go with circular deceleration layers, the dipole being offset from the center. Problem B, a direct problem is to find the deceleration layer that goes with no body. It is felt that this selection is typical, and can be expected to show all the various types of behavior discussed in the preceding section.

Dealing first with problem A, we proceed as follows: We have $s = \theta$ so that x_L, y_L, R, ϕ, B_n and B_s can all be expressed directly in terms of s. With these preliminaries, (6.18) is a single first order differential equation for P(s), while (6.15), (7.6) and (7.8) introduce the auxiliary quantities p_M, I and $\delta(s)$. When this has been solved, M may be found from (7.7), ψ_M from (6.20), and we can then study (6.23). If, for some guessed S and r_s, B_n reaches zero when p_M reaches zero (in accordance with the discussion in the previous section) we have a valid solution, and (6.23) may be solved for $h(\eta)$ which gives the body shape.

The values of S and r_s which result from these calculations are shown on Fig. 7 (marked "circular shock"). It is noteworthy that, as far as the calculation went, a circular deceleration layer always corresponded to a value of r_s close to 0.7 (these remarks refer to the two-dimensional case). It is not easy to see why r_s should be as insensitive as it is over this range, but an explanation along the following lines seems reasonable: If $r_s = 1$, $B_n = 0$ at $\theta = \phi = \pi/2$ as in Fig. 5. With centrifugal forces, the deceleration layer can never reach $\theta = \pi/2$ with $p_M \geq 0$. Therefore, we always expect $r_s < 1$. On the other hand, if B_n is to vanish (i.e. layer and field become parallel) at an angle like one radian, r_s cannot be too small. A second feature to notice in Fig. 7 is the effect of the cube in (7.13). Take $r_s = .7$ for example; we find $r_b/r_s = 0$ for S = 1.6, $r_b/r_s = .5$ for S = 1.4, $r_b/r_s = .75$ for S = 1. In other words, the range of interaction parameters for which r_b/r_s is substantially less than unity is very small. This situation has an important practical consequence. For in some physical situation we could imagine the quantity $\sigma/\rho_\infty u_\infty$ changing by many orders of magnitude. The significance of the cube in (7.13) is then that the change from

quasi-aerodynamic to fully magnetohydrodynamic flow takes place when $\sigma/\rho_\infty u_\infty$ varies only by a factor of 2 or so. Put another way, the fully magnetohydrodynamic case is either "on" or "off" in any physical situation. The cube in (7.13) becomes a seventh power in (A.7.13) so that in the axially-symmetric case the above remarks apply a fortiori.

For illustrative purposes, in the intermediate regime, we have chosen one of the cases from Problem A. The one we have chosen has $r_b/r_s = .5$, $S = 1.4$. The variation of the quantities in the deceleration layer is shown against arc length in Fig. 8. Points to notice in this figure are: p_M and B_n vanish together to a sufficient degree of accuracy; $M \approx \psi_M$ indicating that about half the gas that enters the deceleration layer passes through into the slow flow region. This point is further illustrated in Fig. 9 where the deceleration layer, streamlines, field lines and body shape are all shown. The body shape is re-entrant; this proved to be the case for all the circular shocks studied. The implication of this is that cylindrical bodies do not go with circular shocks. The pressure and density in the gas are both 1/4 roughly on the field line $\eta = .5$. In view of the remarks in the previous section it is likely that Fig. 9 should not be taken too seriously beyond this point. The streamlines are shown in the free stream as well as in the slow flow region; notice the displacement in the deceleration layer.

Turning now to Problem B (no body), the computation is somewhat different; in this case the geometry is initially unknown. With $r_b = 0$, (7.13) is a relation between S and r_s; it is a question of finding which pair of values S and r_s satisfying (7.13) with $r_b = 0$, leads (using $h(\eta) \equiv 0$) to a deceleration layer for which p_M and B_n vanish simultaneously. The result of the calculation was $S = 1.60$, $r_s = .72$. The variation of the properties along the deceleration layer are shown in terms of arc length in Fig. 10, and the slow flow region and overall geometry are shown in Fig. 11. The resultant shock shape is, as can be seen, nearly circular. The limiting streamline is the field line $\eta = .55$. The line is effectively the limit (as $r_b \to 0$) of the re-entrant body shapes typified by the one shown in Fig. 9. The two flows illustrated are clearly not very different. The most import-

a

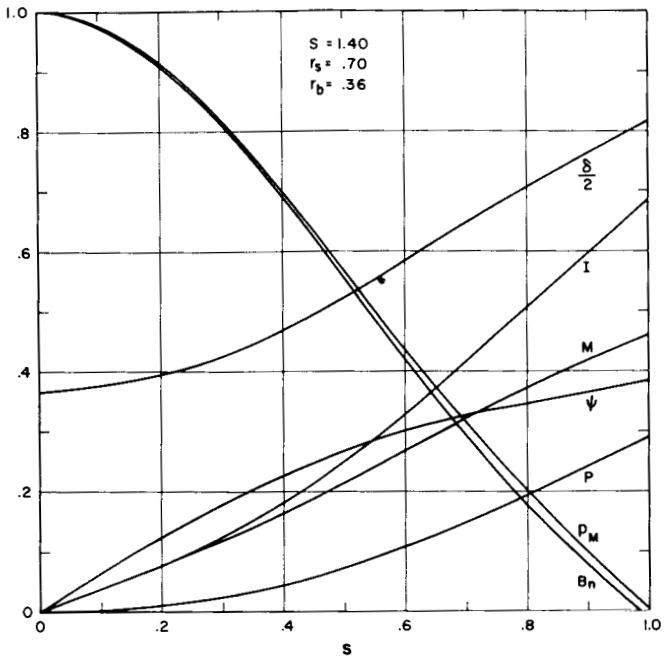

b

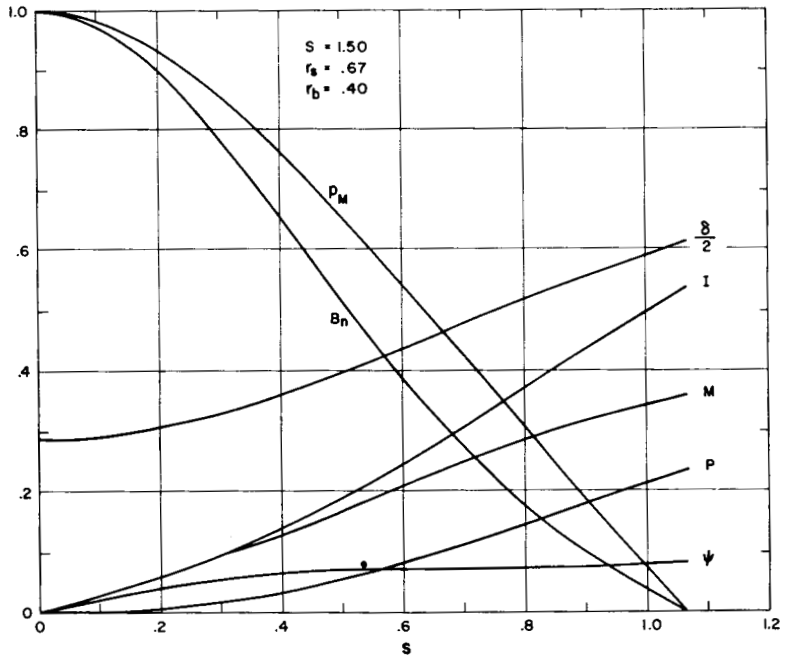

Fig. 8 Shows the variation of significant quantities relevant to the deceleration layer for a typical value of S in the range where the drag is divided between the coil and the body. The abscissa represents arc length along the deceleration layer. p_M and B_n vanish at the same place to a sufficient degree of accuracy.

a

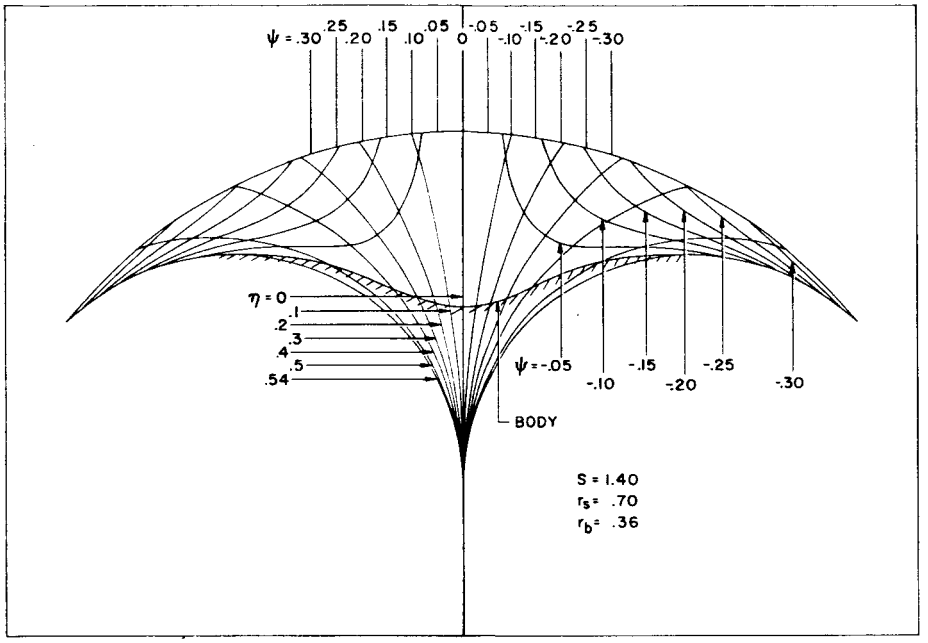

b

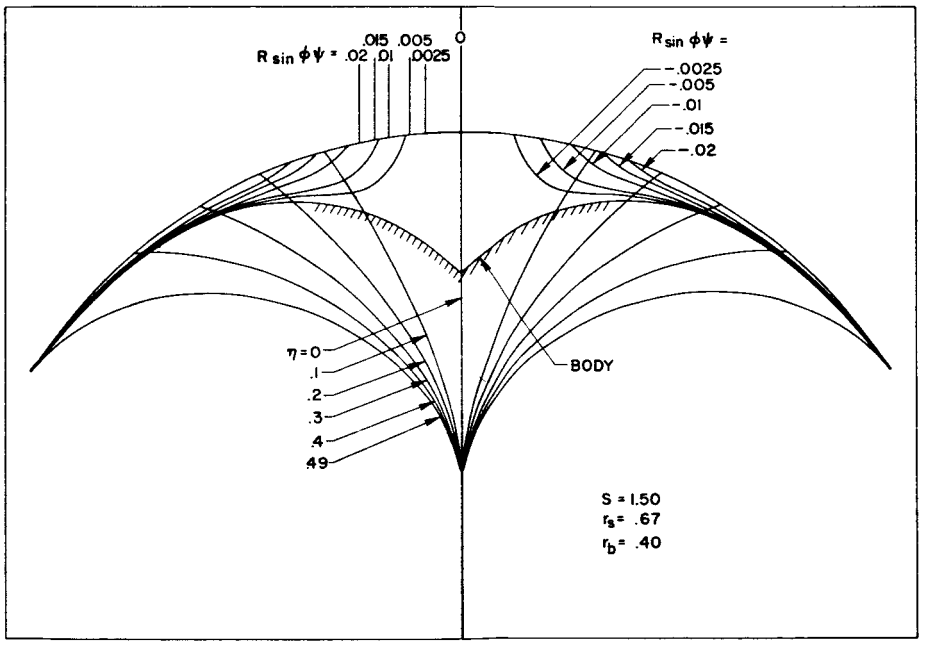

Fig. 9 Represents the streamlines for a typical mixed MHD aerodynamic flow. Equal masses flow between the streamlines shown. Note the displacement of the streamlines in the deceleration layer. The magnetic field lines are also shown. The center of curvature of the shock is at the bottom of the figure. The shape of the body beyond the field line $\eta = .54$ is irrelevant since it is not in contact with the flow.

a

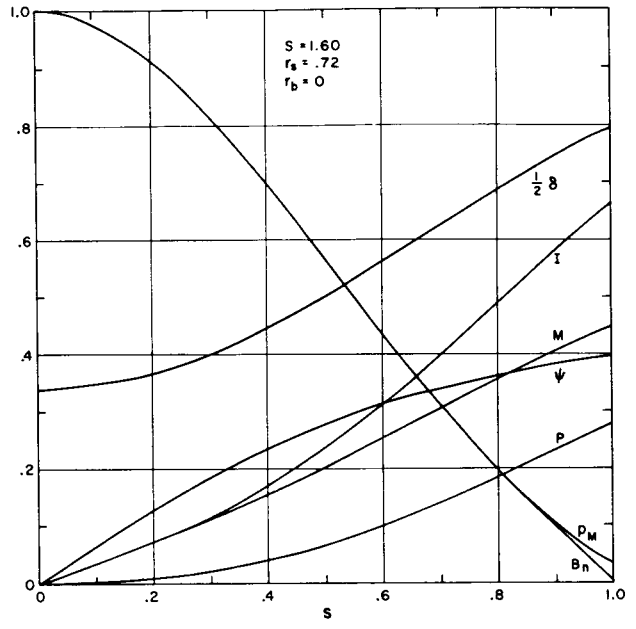

b

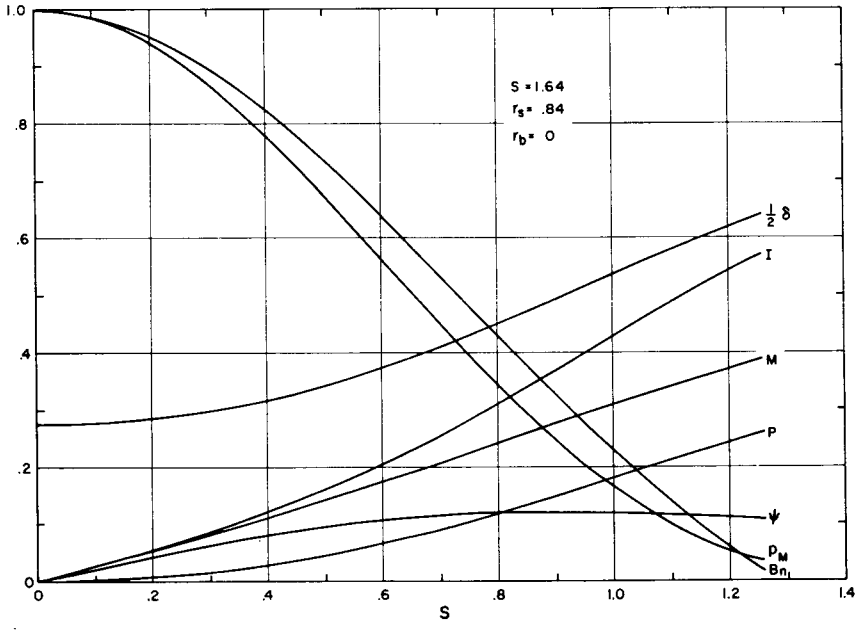

Fig. 10 Shows the variation of the significant quantities relevant to the deceleration layer for the fully magnetohydrodynamic case. The abscissa represents arc length. p_M and B_n vanish at the same place to a sufficient degree of accuracy. In a they are virtually indistinguishable throughout.

a

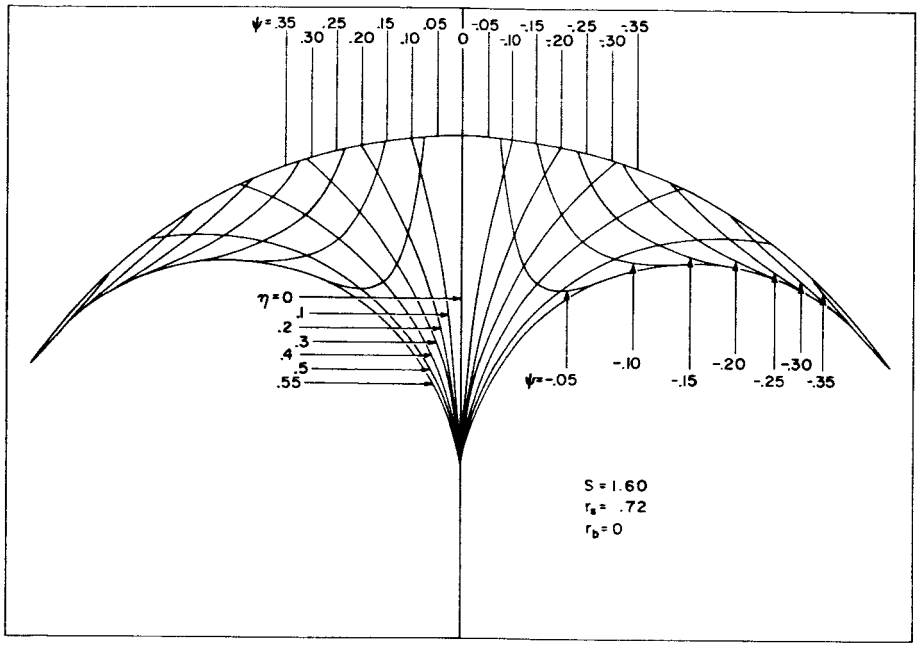

b

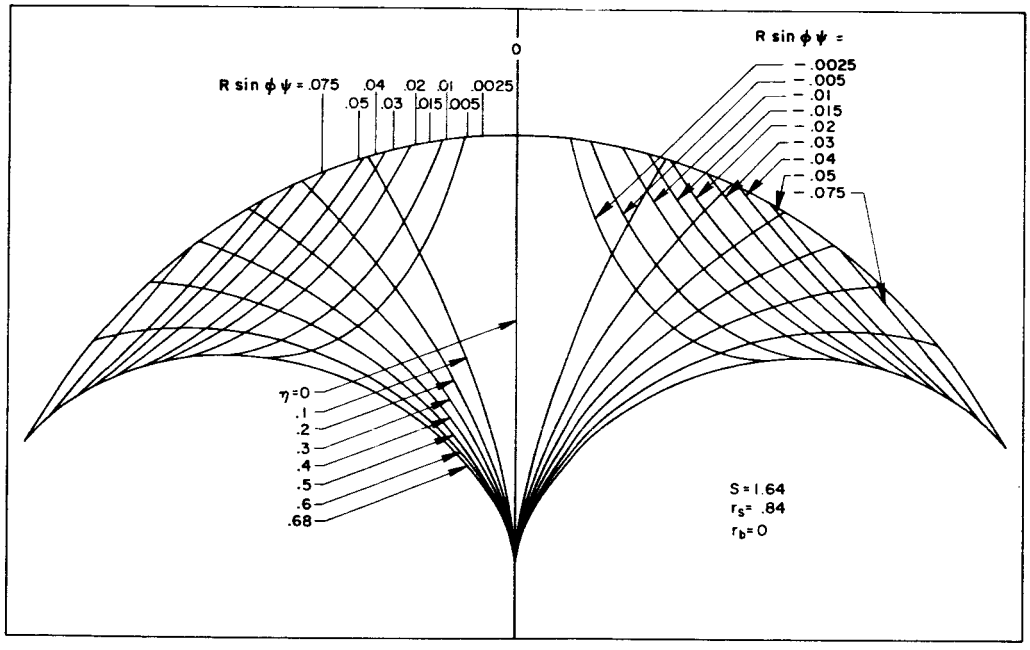

Fig. 11 Represents the streamlines for the fully magnetohydrodynamic flow. Equal masses flow between the streamlines shown. Note the displacement of the streamlines in the deceleration layer. The magnetic field lines are also shown. The center of curvature of the shock is at the bottom of the figure.

ant number to emerge from this analysis however, is the value S = 1.60, for this is the largest possible value of S; any further increase in, say, the conductivity or magnetic moment of the coil, results only in a larger stand-off distance, the value of S being unchanged. As in the case of Fig. 9, Fig. 11 should probably be disregarded beyond about $\eta = .5$, on which field line the pressure and density are about .25. Beyond this field line, Fig. 11 predicts a substantial rise in velocity (coming together of the streamlines) indicating that the low Mach number approximation is no longer valid.

VIII. DISCUSSION AND CONCLUSIONS

The principal result of the foregoing analysis is that when (for the axially symmetric case)

$$S = \epsilon\sigma u_\infty r_c B_o^2/\rho_\infty u_\infty^2 \approx 1.6 \tag{8.1}$$

a flow pattern is set up in which the forces acting on the flow are almost entirely magnetic in origin. Forces exerted at solid surfaces are important only over a negligible area around the stagnation point. The demonstration that this type of flow can exist even at low magnetic Reynolds number was one of our principal objectives. On the other hand, the result (8.1) was not achieved without making a number of assumptions nearly all of which need closer examination if we are to make a more accurate assessment of the physical conditions to which (8.1) should apply. In this section we shall discuss some of these physical conditions and also mention briefly the situation as regards experimental (laboratory) verification of the theoretical work in this area.

We commence with a discussion of the effects of finite (as opposed to vanishingly small) ϵ. In practical situations ϵ may be as small as .05 in which case $\epsilon^{1/4}$ is about .5. This obviously casts a shadow on those parts of the flow picture dependent on $\epsilon^{1/4}$ being small, notably the joining of the deceleration layer to the slow flow region near the sonic points. We feel however that the effect of finite ϵ will be one in which things get "smeared out" rather than fundamentally changed. Most notably, for finite ϵ, the slow flow will require a considerable area to be passed out at sonic speed parallel to the magnetic field. However, the distinction between the deceleration layer and the slow flow region is also less distinct for larger ϵ, so that it seems fair to describe the net effect as one of "blurring" a picture whose sharp outlines are useful for descriptive and mathematical purposes, but not physically realistic.

We turn next to consideration of the Hall effect. When $\omega\tau$ ($\omega = eB/m$,

the electron cyclotron frequency; τ = mean free time between scattering collisions for the electrons) is not small, the electric current is reduced in magnitude and does not flow in the direction of the applied electric field. In some simple cases, the angle between the current and the applied field is just $\tan^{-1} \omega\tau$. However, cases can arise in which the angle between the current and the electric field remains small and the magnitude of the current stays the same even though $\omega\tau$ grows to values in excess of unity. Just such a case arose in the paper of Levy and Petschek.[4] Here the Hall currents (roughly the component of the electric current perpendicular to the electric field) were restricted to flow in a long narrow region of aspect ratio ϵ. This inhibited them to the extent that no important effect was noted until $\omega\tau$ grew to values in excess of ϵ^{-1}. This case does not occur in the present geometry; the Hall currents would flow, in this case, throughout the slow flow region. For this reason, the result (8.1) can be expected to hold only for values of $\omega\tau$ less than unity. Toward the edge of the slow flow region $\omega\tau$ will rise considerably due to the decrease in the gas density. Thus the Hall effect will limit the sharpness of the boundary to the slow flow region. A similar effect is ion slip, which occurs when the density is so low that the neutrals can leak past the ions. The presence of ion slip would result in some small heat transfer to those parts of the surface of the body which the ideal theory shows to be not in contact with the hot gas.

A further physical limitation is that of chemical non-equilibrium. At sufficiently low density there may not be time for the ionization processes in the gas to reach equilibrium. Thus Boyer[9] claims that non-equilibrium effects make the attainment of substantial interaction parameters in hypersonic wind tunnel facilities problematical for unseeded air. For the flight case, it is probably fair to say that where non-equilibrium effects are important, the density must be so low as to preclude useful dynamic effects. However, it is difficult to generalize on this subject and we must usually be content with calculating the magnitude of likely effects in any given case.

A final limitation on the physical realizability of the flows discussed in this paper arises from the following consideration. The gas ahead of the strong shock is supposed to be cold and unionized, a condition which is cer-

tainly met in the planetary entry case. However, the magnetic field of the coil extends substantially beyond the shock and the cold gas therefore "sees" an effective electric field. The question arises as to whether this electric field is sufficient to break down the gas. This question is quite involved, and is discussed at the end of the paper of Levy and Petschek.[4] On the one hand arguments can be given to show that breakdown could not occur for velocities less than about 5×10^6 cm/sec, i.e. about 5 times satellite velocity. On the other hand, unanswered questions remain having to do with the possibility of substantial photo ionization in the gas ahead of the shock.

This comment about photo ionization introduces the subject of radiant heat transfer. It has been shown, for instance by Goulard,[10] that the magnetohydrodynamic interaction can sometimes increase the radiant heat transfer to a body while decreasing the convective heat transfer, the flow conditions remaining fixed. This effect is due to the increased volume of hot radiating gas that is a consequence of the increase in the stand-off distance. Since in this paper we deal only with the dynamics of the flow, and since under ordinary conditions radiation does not affect the dynamics of this type of flow we shall not pursue this subject here. It does seem worth pointing out however, that for a fixed object re-entry may take place at a higher altitude due to dynamic effects. Thus the radiant heat transfer to a body could be reduced by causing it to decelerate at a higher altitude.

We conclude by reviewing the status of quantitative experiment in the field of low magnetic Reynolds number hypersonic flows. Early work in the field by Bush and Ziemer[11] appeared to give good results, but a recent article by Cloupeau[12] appears to throw some doubt on the quantitative interpretation of results achieved in electromagnetic shock tubes of the type used by Bush and Ziemer. Work on this subject has also been reported by Wilkinson[13] and Ericson et al[14] although neither of these studies appears to have given very good results. We understand that a description by Locke, Petschek and Rose[15] of experimental work performed by them with the object of verifying the existence of fully magnetohydrodynamically supported hypersonic flows (as predicted by Levy and Petschek[4]) is forthcoming. Preliminary results indicate that such flows can be supported with negligible physical contact between the hot gas and solid surfaces.

ACKNOWLEDGMENTS

The authors wish to express appreciation to H. E. Petschek for helpful suggestions during the course of this work.

APPENDIX

Axially Symmetric Case

The axially symmetric equation of continuity in the shock layer is

$$\frac{\partial(\rho u)}{\partial \tilde{r}} = \frac{1}{\sin\theta} \frac{\partial}{\partial \theta} (\rho v \sin\theta) \qquad \text{(A. 3. 4)}$$

and on the stagnation streamline this reduces to

$$\frac{d(\rho u)}{d\tilde{r}} = 2\rho \frac{\partial v}{\partial \theta} \qquad \text{(A. 3. 5)}$$

When $\rho = 1$ this gives

$$\frac{du}{d\tilde{r}} = 2\frac{\partial v}{\partial \theta} \qquad \text{(A. 3. 13)}$$

The momentum and energy equations are unchanged. Integration along the stagnation streamline proceeds as follows:

$$\frac{\partial v}{\partial \theta} \frac{d\tilde{r}}{u} = \frac{1}{2} \frac{du}{u} = \frac{d\left(\frac{\partial v}{\partial \theta}\right)}{\frac{\partial v}{\partial \theta} + S} \qquad \text{(A. 3. 19)}$$

Hence

$$(-u)^{1/2} = \left(\frac{\partial v}{\partial \theta} + S\right)\left(1 + S\right)^{-1} \qquad \text{(A. 3. 20)}$$

The profiles of $-u$ and $\partial v/\partial \theta$ as functions of $\tilde{r}$ cannot be written explicitly. However, we can derive the following implicit expressions:

$$\left.\begin{aligned} \tilde{r} &= \frac{(1-\sqrt{-u})}{1+S} - \frac{S}{(1+S)^2} \ln\left[\sqrt{-u}\,(1+S) - S\right] \\ \tilde{r} &= \left[\left(1 - \frac{\partial v}{\partial \theta}\right) - S \ln \frac{\partial v}{\partial \theta}\right] (1+S)^{-2} \end{aligned}\right\} \qquad \text{(A. 3. 21)}$$

These profiles resemble their two-dimensional analogues in the essential respect that $\partial v/\partial \theta$ approaches zero and $-u$ approaches a finite limit exponentially. • The limit approached by $-u$ is $S^2(1+S)^{-2}$.

The arguments given to prove that $S\epsilon^{-1/2} \approx 1$ divides two flow

regimes carry over unchanged to this case. The transverse pressure gradient in the layer is given in terms of $\partial v/\partial\theta$ by:

$$\frac{-\partial^2 p}{\partial\theta^2} = 2 + \frac{\frac{2}{3}\left[1-\left(\frac{\partial v}{\partial\theta}\right)^3\right]}{(1+S)^2} + \frac{S\left[1-\left(\frac{\partial v}{\partial\theta}\right)^2\right]\left[1+\frac{\partial B_\theta}{\partial\theta}\right]}{(1+S)^2} + \frac{2S^2\left[1-\frac{\partial v}{\partial\theta}\right]}{(1+S)^2}\frac{\partial B_\theta}{\partial\theta} \quad \text{(A. 3. 22)}$$

At the back of the layer this is:

$$k = \left.\frac{-\partial^2 p}{\partial\theta^2}\right|_{\substack{\theta = o \\ \tilde{r} = \infty}} = 2 + \frac{2/3}{(1+S)^2} + \frac{S\left[1+\frac{\partial B_\theta}{\partial\theta}\right]}{(1+S)^2} + \frac{2S^2\,\frac{\partial B_\theta}{\partial\theta}}{(1+S)^2} \quad \text{(A. 3. 23)}$$

In this expression the last two terms represent the magneto-hydrodynamic effect. For the dipole as shown in Fig. 2

$$\left.\frac{\partial B_\theta}{\partial\theta}\right|_{\text{stag. pt.}} = \frac{3-2r_s}{2r_s} \quad \text{(A. 3. 24)}$$

The aerodynamic (S = 0) value of k is 8/3 (A. 3. 23), and the reduction in the stagnation point velocity ratio is therefore:

$$\left(\frac{8}{3}\epsilon\right)^{-1/2}\frac{\partial v}{\partial\theta} = \frac{-S}{\sqrt{32\epsilon/3}} + \sqrt{\frac{3S^2}{32\epsilon} + \frac{3k}{8}} \quad \text{(A. 3. 26)}$$

The non-magnetic stand-off distance is $\epsilon\left[1+(8\epsilon/3)^{1/2}\right]^{-1}$ and Δ is given by

$$\frac{\Delta}{\epsilon} = \frac{1}{2Q_o}\left(\frac{Q_o-Q_1}{1-Q_1}\right)^2 F\left[2, \frac{Q_o+Q_1}{Q_o-Q_1}+1, \frac{Q_o+Q_1}{Q_o-Q_1}+2; \frac{1-Q_o}{1-Q_1}\right] \quad \text{(A. 3. 27)}$$

F is once more the hypergeometric function. The definitions of Q_o and Q_1 and a are unchanged. The back of the deceleration layer is defined for the axially symmetric case as the place where $-u = S^2(1+S)^{-2}$, and this value has been used in constructing Fig. 4b.

Turning now to the slow flow region in the axially symmetric case, the radial and tangential velocity components are given in terms of the stream function by:

$$-\frac{1}{\rho R}\sin\phi\,\frac{\partial}{\partial\phi}(\psi\sin\phi),\ \frac{1}{\rho R}\frac{\partial}{\partial R}(\psi R) \qquad \text{(A. 4. 4)}$$

Note that this stream function is defined like a vector potential, that is to say, the mass flow vector is represented as the curl of a vector of magnitude ψ pointing in the azimuthal direction. Thus, the streamlines are represented not by ψ = constant, but by R $\sin\phi\,\psi$ = constant. The choice of definition is, of course, arbitrary, but the distinction must be remembered when plotting streamlines.

The field components are

$$\underset{\sim}{B} = \left(\frac{r_s}{R}\right)^3 \cos\phi,\ \frac{1}{2}\left(\frac{r_s}{R}\right)^3 \sin\phi \qquad \text{(A. 4. 6)}$$

The components of (4. 5) are

$$\frac{1}{2}\frac{\partial p^2}{\partial R} = \frac{S}{2}\left(\frac{r_s}{R}\right)^6 \sin\phi\left[\frac{\cos\phi}{R}\frac{\partial}{\partial R}(R\psi) + \frac{1}{2R}\frac{\partial}{\partial\phi}(\psi\sin\phi)\right] \qquad \text{(A. 4. 7)}$$

$$\frac{1}{2R}\frac{\partial p^2}{\partial\phi} = -S\left(\frac{r_s}{R}\right)^6 \cos\phi\left[\frac{\cos\phi}{R}\frac{\partial}{\partial R}(R\psi) + \frac{1}{2R}\frac{\partial}{\partial\phi}(\psi\sin\phi)\right] \qquad \text{(A. 4. 8)}$$

Multiply (A. 4. 7) by $\cos\phi$, (A. 4. 8) by $\frac{1}{2}\sin\phi$ and add:

$$\frac{1}{2}\left[\cos\phi\frac{\partial}{\partial R} + \frac{1}{2}\frac{\sin\phi}{R}\frac{\partial}{\partial\phi}\right]p^2 = 0 \qquad \text{(A. 4. 9)}$$

This equation implies that p is a function only of

$$\eta = \frac{r_s^2\sin^2\phi}{R} \qquad \text{(A. 4. 10)}$$

Once again this states only that the pressure is constant along field lines. Now multiply (A. 4. 7) by $\sin\phi$, (A. 4. 8) by $\frac{1}{2}\cos\phi$ and subtract:

$$\left[\sin\phi\frac{\partial}{\partial R} - \frac{\cos\phi}{2R}\frac{\partial}{\partial\phi}\right]p^2 = S\left(\frac{r_s}{R}\right)^6\left[\frac{\cos\phi}{R}\frac{\partial}{\partial R}(R\psi) + \frac{1}{2R}\frac{\partial}{\partial\phi}(\psi\sin\phi)\right] \qquad \text{(A. 4. 11)}$$

Using the fact that $p = p(\eta)$, the left hand side of this is equivalent to

$-\frac{1}{2}\sin\phi\left(\frac{r_s}{R}\right)^2\frac{dp^2}{d\eta}$, so that

$$-\sin\phi \frac{dp^2}{d\eta} = S\left(\frac{r_s}{R}\right)^4 \left[\frac{\cos\phi}{R} \frac{\partial}{\partial R}(R\psi) + \frac{1}{2R} \frac{\partial}{\partial \phi}(\psi \sin\phi)\right] \quad (A.4.12)$$

In view of the fact that $dp^2/d\eta$, like p, is a function of η alone, we can find solutions of (A.4.12) of the form:

$$\psi = -\frac{1}{S} \frac{dp^2}{d\eta} G(R, \phi) \quad (A.4.13)$$

G satisfies the equation:

$$\left(\frac{r_s}{R}\right)^4 \left[\frac{\cos\phi}{R} \frac{\partial}{\partial R}(GR) + \frac{1}{2R} \frac{\partial}{\partial \phi}(G \sin\phi)\right] = \sin\phi \quad (A.4.14)$$

A particular solution of this equation may be found in the form:

$$G = \frac{R^5}{r_s^4} g(\phi) \quad (A.4.15)$$

where g satisfies

$$\sin\phi\, g' + 13\, g \cos\phi = 2 \sin\phi \quad (A.4.16)$$

The solution of this equation finite at $\phi = 0$ is

$$g = \frac{2\int_0^\phi \sin^{13} t\, dt}{\sin^{13}\phi} \quad (A.4.17)$$

In addition, any function $(R \sin\phi)^{-1} h(\eta)$ satisfies the homogeneous part of (A.4.14) so that the general solution of the problem is

$$\psi = -\frac{1}{S} \frac{dp^2}{d\eta} \frac{1}{R\, r_s^4 \sin\phi} \left[\frac{2R^6}{\sin^{12}\phi} \int_0^\phi \sin^{13} t\, dt + \eta\, h(\eta)\right] \quad (A.4.18)$$

In general, $\eta\, h(\eta)$ can be chosen so that any body is given by $\psi = 0$. This form is chosen so that when $\phi \to 0$ the two terms in the brace behave similarly. We restrict ourselves to a spherical body R = a, and find

$$h\left(\frac{r_s^2 \sin^2\phi}{a}\right) + \frac{2a^6}{\sin^{12}\phi} \int_0^\phi \sin^{13} t\, dt = 0 \quad (A.4.19)$$

$$h(\eta) = -2\, r_s^{12}\, \eta - 6 \int_0^{\sin^{-1}\left(\frac{\sqrt{a\,\eta}}{r_s}\right)} \sin^{13} t\, dt \qquad (A.4.20)$$

giving finally,

$$\psi(R,\phi) = -\frac{1}{S}\frac{dp}{d\eta}^2 \cdot \frac{2R^5}{r_s^4 \sin^{13}\phi} \int_{\sin^{-1}\left(\sqrt{\frac{a}{R}}\,\sin\phi\right)}^{\phi} \sin^{13} t\, dt \qquad (A.4.21)$$

If for illustrative purposes we assume a hemispherical shock centered at the dipole so that $r_s = 1$ and also that $p = \cos^2\phi$ on it, then, through the flow field p would be given by

$$p = p(\eta) = 1 - \eta \qquad (A.4.22)$$

The remarks concerning Fig. 5a in the text apply equally to Fig. 5b. Note that lines of constant $\psi R \sin\phi$ (rather than constant ψ) are shown.

For the axially symmetric case, matching on the stagnation streamline proceeds as follows: the pressure is given from (A.3.23) and may be written

$$p \approx 1 - \frac{1}{2} k\theta^2 \qquad (A.5.1)$$

valid at the back of the deceleration layer for small θ. In this region the field line parameter η is given from (A.4.10) by

$$\eta \approx r_s \phi^2 \approx \frac{1}{r_s}\theta^2 \qquad (A.5.2)$$

Hence,

$$p \approx 1 - \frac{1}{2} k\, r_s\, \eta \qquad (A.5.3)$$

The stream function in this region is, from (A.4.18),

$$\psi \approx \frac{r\,\theta k}{S\, r_s^3}\left[\frac{R^4}{7} + \frac{h(o) r_s^2}{R^3}\right] \qquad (A.5.4)$$

The radial velocity at the shock is given by:

$$u \approx -\frac{1}{\rho r_s \phi}\frac{\partial}{\partial\phi}(\psi\,\phi) \approx -\frac{1}{\theta}\frac{\partial}{\partial\theta}(\psi\theta)\Bigg|_{\substack{\theta = 0 \\ r = 1}} \qquad (A.5.5)$$

and this must be matched to the back of the shock layer as given in (A. 3. 21). We find

$$\left(\frac{S}{1+S}\right)^2 = \frac{2k}{Sr_s^3}\left[\frac{r_s^4}{7} + \frac{h(o)}{r_s}\right] \qquad (A.5.6)$$

This yields:

$$21S^3 - [18S^2 + (24r_s + 9)S + 16r_s]\left[1 + \frac{7h(o)}{5r_s}\right] = 0 \qquad (A.5.7)$$

The body is given by:

$$\frac{r_b^4}{7} + \frac{r_s^2}{3r_b}h(o) = 0 \qquad (A.5.8)$$

and, therefore,

$$21S^3 - [18S^2 + (24r_s + 9)S + 16r_s]\left[1 - \left(\frac{r_b}{r_s}\right)^7\right] = 0 \qquad (A.5.9)$$

Δ, defined as in (5.10) is given by

$$\Delta = \left[1 - \frac{21S^3}{18S^2 + (24r_s + 9)S + 16r_s}\right]^{-1/7} - 1 \qquad (A.5.11)$$

The fully magnetohydrodynamic case is given by:

$$21S^3 - 18S^2 - (24r_s + 9)S - 16r_s = 0 \qquad (A.5.12)$$

For the special assumption $r_s = 1$, this equation has the root $S = 1.90$.

Turning now to the axially symmetric deceleration layer away from the stagnation streamline, the n and s coordinate system (Fig. 6) is unchanged, and equations (6.1) through (6.4) remain valid. The equation of continuity, however, now reads

$$\frac{\partial(\rho u)}{\partial \tilde{n}} - \frac{1}{y_L}\frac{\partial}{\partial s}(\rho v y_L) = 0 \qquad (A.6.5)$$

The field components B_s and B_n are given in terms of B_x and B_y by (6.7), but B_x and B_y are now given by:

$$\left.\begin{aligned} B_x &= \frac{1}{4}\left(\frac{r_s}{R}\right)^3 (1 + 3\cos 2\phi) \\ B_y &= \frac{3}{4}\left(\frac{r_s}{R}\right)^3 \sin 2\phi \end{aligned}\right\} \qquad (A.6.8)$$

All the equations (6.9) through (6.16) carry over unchanged to the axially symmetric case, including the important definitions (6.14), and the integrated normal momentum equation (6.15). (6.16) becomes, on using the continuity equation (A.6.5)

$$\dot{x}_L \dot{y}_L + \frac{1}{y_L}\frac{d}{ds}(P y_L) + S B_n^2 I = 0 \qquad (A.6.18)$$

We define the stream function by:

$$\rho u = -\frac{1}{y_L}\frac{\partial}{\partial s}(\psi y_L); \rho v = -\frac{\partial \psi}{\partial \tilde{n}} \qquad (A.6.19)$$

At the shock, $\psi = \frac{1}{2} y_L$, and integration of the second equation (A.6.19) through the layer yields

$$M = \frac{1}{2} y_L - \psi_M \qquad (A.6.20)$$

The axially symmetric Busemann relation is found from (6.15) and (A.6.18) by setting S = 0:

$$p_M = \dot{y}^2 + \frac{\kappa}{y_L}\int_0^s \dot{x}_L \dot{y}_L y_L \, ds \qquad (A.6.21)$$

On the deceleration layer, using η as given by (A.4.10) we find:

$$\frac{d\eta}{ds} = \frac{2R}{r_s}\sin\phi \, B_n \qquad (A.6.22)$$

so that (A.4.18) becomes

$$\psi_M = -\frac{p_M}{SB_n}\frac{dp_M}{ds}\left[\frac{2R^4}{r_s^3}\frac{\int_0^\phi \sin^{13} t \, dt}{\sin^{14}\phi} + \frac{h(\eta)}{r_s R^3}\right] \qquad (A.6.23)$$

For the numerical calculations, equation (7.1) through (7.8) are unchanged in the axially symmetric case. However, (A.6.18) yields:

$$\delta_o = \frac{2}{S+2} \tag{A.7.9}$$

(6.15) yields:

$$k = 2 + \delta_o \left[\frac{2}{3} + S\left(\frac{3}{2r_s} - 1\right)\right] \tag{A.7.10}$$

Substitution from (A.7.9) gives

$$k = 2 + \frac{4/3}{S+2} + \frac{2S}{S+2}\left[\frac{3}{2r_s} - 1\right] \tag{A.7.11}$$

which should be compared with (A.3.23). From (A.6.20), for small s, we find

$$\psi_M \approx \frac{\frac{1}{2}S}{S+2}\, s \tag{A.7.12}$$

and from (A.6.23)

$$21S^2 - (32r_s + 18S)\left[1 - \left(\frac{r_b}{r_s}\right)^7\right] = 0 \tag{A.7.13}$$

(A.7.13) and (A.5.9) are compared in Fig. 7b.

REFERENCES

1. Kemp, N. H., "On Hypersonic Stagnation Point Flow with a Magnetic Field," J. Aeronautical Sciences, Readers' Forum, 25, 6, 405-407, June 1958. See also Freeman, N. C., "On the Flow Past a Sphere at Hypersonic Speed with a Magnetic Field," J. Aero/Space Sciences, 26, 10, 670-672, October 1959 and Kemp, N. H., "Author's Reply," J. Aero/Space Sciences, 26, 10, 672, October 1959.
2. Bush, W. B., "Magnetohydrodynamic-Hypersonic Flow Past a Blunt Nose," J. Aero/Space Sciences, 25, 11, 685-690, November 1958. See also Bush, W. B., "A Note on Magnetohydrodynamic-Hypersonic Flow Past a Blunt Body," J. Aero/Space Sciences, 26, 8, 536, August 1959.
3. Lykoudis, P. S., "The Newtonian Approximation in Magnetic Hypersonic Stagnation-Point Flow," J. Aero/Space Sciences, 28, 7, 541-546, July 1961.
4. Levy, R. H. and Petschek, H. E., "Magnetohydrodynamically Supported Hypersonic Shock Layer," Phys. Fluids, 6, 7, 946-961, July 1963.
5. Hayes, W. D. and Probstein, R. F., Hypersonic Flow Theory (Academic Press, New York, 1959).
6. Li, T. Y. and Geiger, R. E., "Stagnation Point of a Blunt Body in Hypersonic Flow," J. Aeronaut. Sci. 24, 25 (1957).
7. Pohlhausen, K., "Zur naherungsweisen Integration der Differentialgleichung der laminaren Reibungsschicht," Z. angew. Math. Mech., 1, 252 (1921).
8. Busemann, A., "Flussigkeits-und-Gasbewegung," Handworterbuch der Naturwissenschaften, Vol. IV, 2nd Ed., pp. 244-279. Gustav Fischer, Jena, 1933.

9. Boyer, D. W., "Ionization Nonequilibrium Effects on the Magnetogasdynamic Interaction in the Stagnation Region of an Axisymmetric Blunt Body," Cornell Aeronautical Laboratory report No. AG-1547-Y-1, June 1963.

10. Goulard, R., "An Optimum Magnetic Field for Stagnation Heat Transfer Reduction at Hypersonic Velocities," Bendix Products Division, Applied Sciences Laboratory, South Bend, Indiana, February 1959.

11. Bush, W. B. and Ziemer, R. W., "Magnetic Field Effects on Bow Shock Stand-Off Distance," Phys. Rev. Letters, 1, 58, July 1958.

12. Cloupeau, M., "Interpretation of Luminous Phenomena Observed in Electromagnetic Shock Tubes," Phys. Fluids, 6, 5, 679-688, May, 1963.

13. Wilkinson, J. B., "Magnetohydrodynamic Effects on Stagnation-Point Heat Transfer from Partially Ionized Nonequilibrium Gases in Supersonic Flow," AeroChem TP-43, AeroChem Research Laboratories, Inc., Princeton, N.J., March 1962.

14. Ericson, W. B., Maciulaitis, A., Spagnolo, R. A., Loeffler, A. L., Scheuing, R. A., Hopkins, H. B., "An Investigation of Magnetohydrodynamic Flight Control," Grumman Aircraft Engineering Corp., Bethpage, New York, May 1962.

15. Locke, E. V., Petschek, H. E. and Rose, P. H., "Experiments with Magnetohydrodynamically-Supported Shock Layer," To be published.